July 12, 2022

IMAGING EM BARREL CALORIMETER

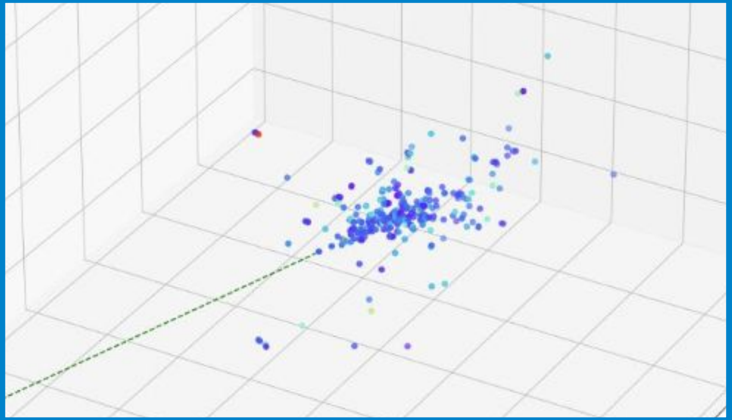

Maria ŻUREK, Argonne National Laboratory

EIC Calorimetry Requirements
Barrel CAL in EIC Yellow Report

EIC Community outlined physics, detector requirements, and evolving detector concepts in the EIC Yellow Report.

EIC Yellow Report requirements for barrel ECal

- Detection of electrons/photons to measure **energy and position**
- Require **moderate energy resolution**
  $(10 - 12)\ \%/\sqrt{E} \oplus (1 - 3)\%$
  - But! With high electron-pion separation at low momenta.
- Require **electron-pion separation up to 10^4** at low particle momenta
- Discriminate between **π^0 decays and single photons** from DVCS
- **Low energy photon** reconstruction ~100 MeV

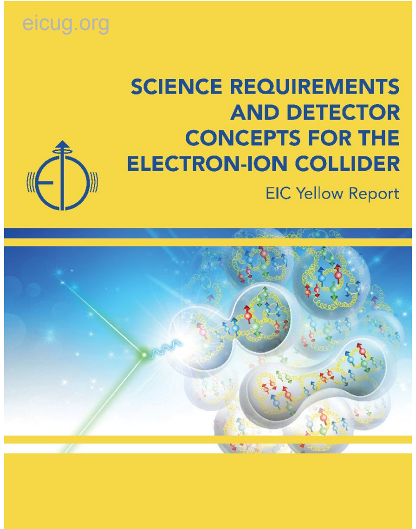

DETECTOR GEOMETRY
Imaging Barrel ECal

https://anl.box.com/s/w5i3e7cmzgznnl1qyjukuhspsn87zwhe

- **Hybrid concept**
  - Imaging calorimetry based on monolithic silicon sensors AstroPix (NASA's AMEGO-X mission)
    Nuclear Inst. and Methods in Physics Research, A 1019 (2021) 165795
  - Scintillating fibers embedded in Pb (Pb/ScFi – Similar to GlueX Barrel ECal)
    Nuclear Inst. and Methods in Physics Research, A 896 (2018) 24-42
- 6 layers of imaging Si sensors interleaved with 5 Pb/ScFi layers and followed by a large chunk of Pb/ScFi section
- Total radiation thickness of 20 X_0
- Detector coverage: $-1.5 < \eta < 1.2$ which overlaps with "electron-going" side endcap

Imaging layer – Position info
Pb/ScFi layer – Energy info

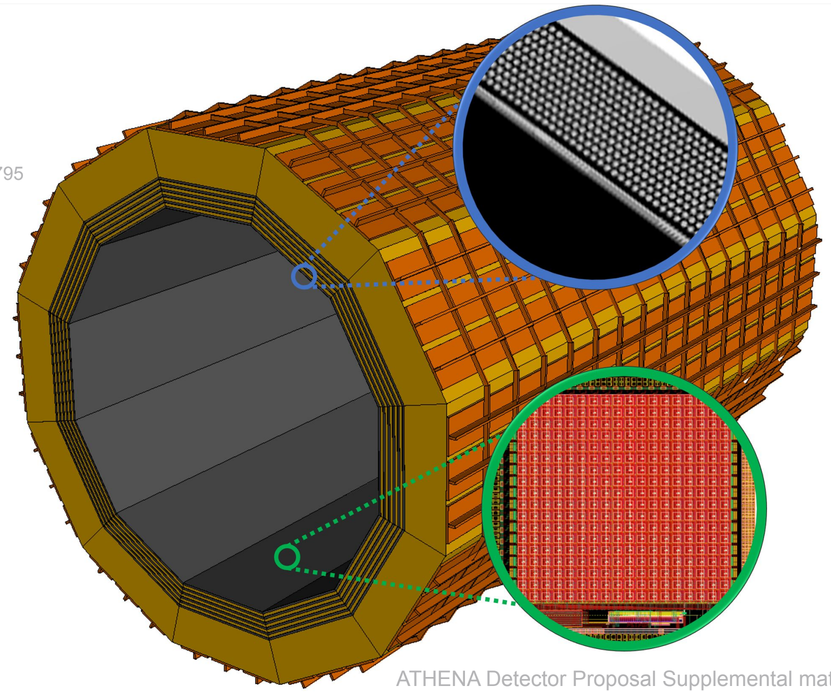

ATHENA Detector Proposal Supplemental material

Performance studies

Imaging Layers in Barrel ECAL

Excellent position resolution allowing precise 3D shower imaging

Significantly improved **electron/pion separation** with respect to E/p method

- Impact on DIS cross section and asymmetries

Separation of ɣs from π^0 decays at high momenta up to ~40 GeV/c. Precise position reconstruction of **ɣs** (below 1 mm at 5 GeV).

- Impact on DVCS and photon physics

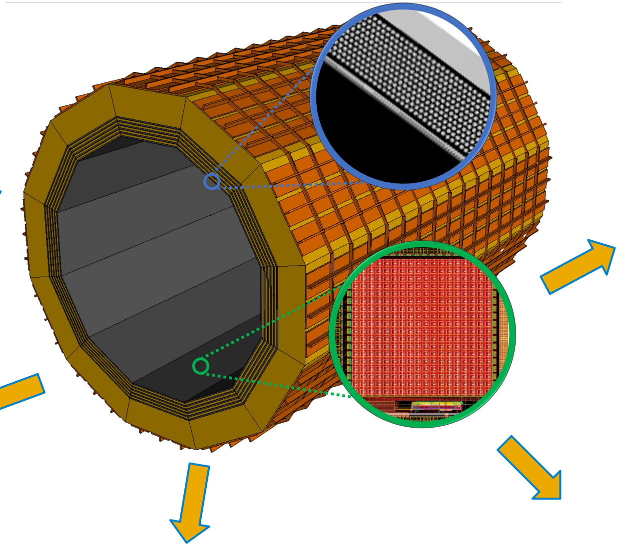

Tagging **final state radiative photons** from nuclear/nucleon elastic scattering at low x to **benchmark QED internal corrections**

Imaging layers provide:

- precise measurement of photon coordinates and the angle between electron and photon

Allowing PID of **low energy muons** that curl inside the barrel ECal (< 1.5 GeV with 3T field)

- Impact on J/psi reconstruction, TCS

Provides a **space coordinate for DIRC** reconstruction (no need for additional large-radius tracking detector)

- Improving PID for SIDIS and beyond
- Improved tracking resolution for high-momentum particles

Imaging Barrel ECal

I. Brewer, et al., arXiv:2101.02665 [astro-ph.IM]

Imaging layers based on **AstroPix** sensors

- Developed for AmegoX NASA mission; successor of ATLASpix (arxiv:2109.13409).

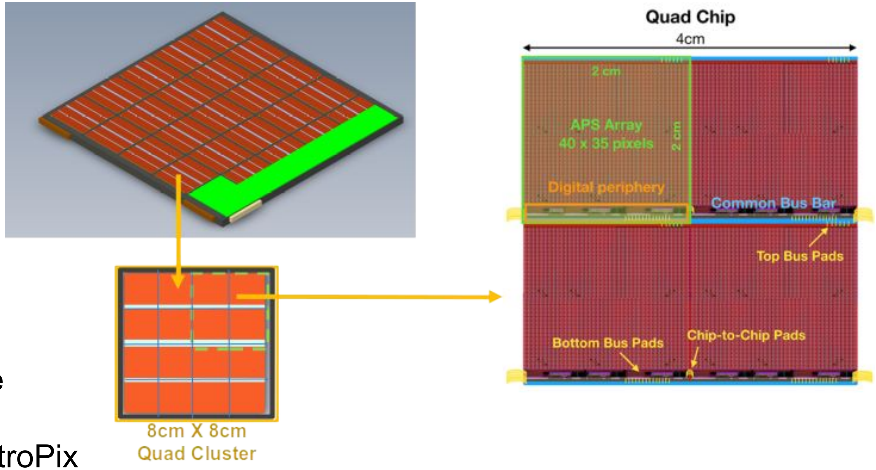

Simulation conditions:

- Digitization on the level of AstroPix pixel
- 4σ threshold cut applied
- No cracks/non-sensitive regions in the sensor coverage assumed in simulations
- In simulations we explore the possibility of using the AstroPix sensor off-the-shelf
- Layer thickness 0.155 cm + 1 cm of air (cooling):

Layer material	Thickness (cm)
Silicon (sensors)	0.05
Silicon (electronics)	0.015
Copper (cables)	0.01
Kapton (insulation)	0.02
Epoxy (glue)	0.01
Carbon (support structure)	0.05

Pixel size	$500\,\mu m \times 500\,\mu m$
Power usage	< 1 mW/cm^2
Energy resolution	10% @ 60 keV (based on the noise floor of 5 keV)
Dynamic range	~ 700 keV
Passive material	$< 5\%$ on the active area of Si
Time resolution	25 ns
Si Thickness	$500\,\mu m$
Time tag	$\sim 1\,\mu$m

Barrel ECal - SciFi/Pb geometry

Pb/ScFi layers follow the GlueX Barrel Calorimeter geometry

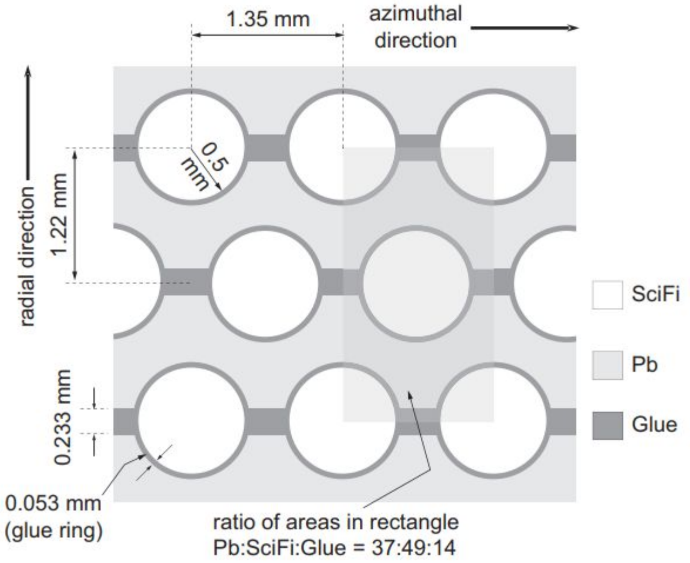

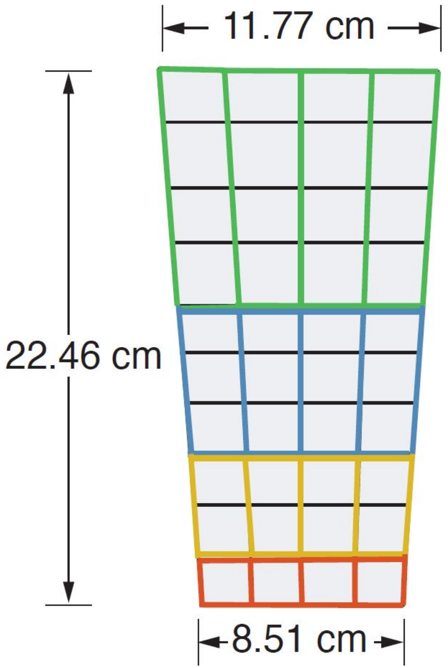

Simulation conditions

- Digitization in simulations on the level of SiPM grid
- Assumed ~ 2 cm x 2 cm grid size
- Possibility of 2-side readout (spatial resolution). In simulations only one side readout for island clustering (no resolution in z)
- Description of clustering algorithms in backup slide
- Birks constant for ScFi k_B = 0.126 mm/MeV

2-side readout in final design; GlueX position resolution in z: 1.1cm/√E [2]

1) Nucl. Instrum. Meth. A, vol. 896, pp. 24–42, 2018, 2) Nucl. Instrum. Meth. A, vol. 596, pp. 327–337, 2008

ENERGY RESOLUTION

The main role of the Pb/ScFi Layers

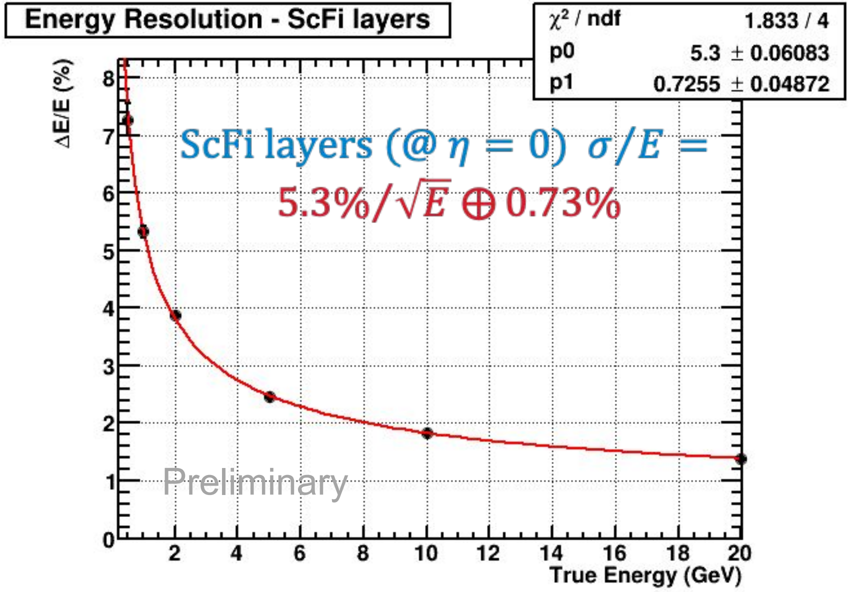

(GlueX ScFi ECal $\sigma/E = 5.2\%/\sqrt{E} \oplus 3.6\%$)

Used 5 GeV γs

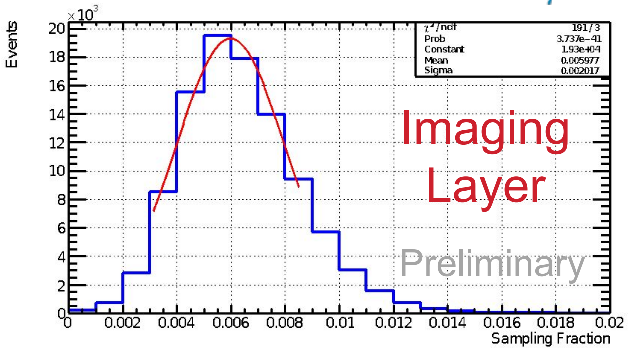

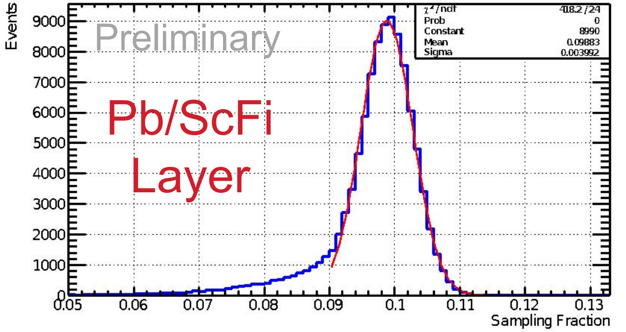

Sampling Fraction$=\dfrac{\sum E_{\text{active layer}}}{E_{\text{thrown}}}$

Imaging Layer ~0.6%

Pb/ScFi Layer ~10%

SPATIAL RESOLUTION

The main role of the Imaging Layers

Cluster level: $\sigma_{\text{spatial}} = (2.32 \pm 0.06)\text{mm}/\sqrt{E} \oplus (1.4 \pm 0.02)\text{mm} \quad @\,\eta = 0$

With first layer hit position on top of cluster level: $\sigma_{\text{spatial}} =$ 0.5mm (i.e. pixel size)

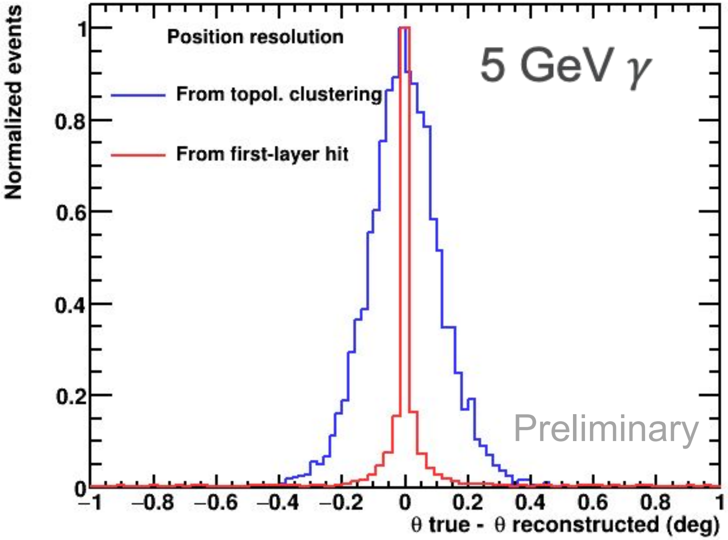

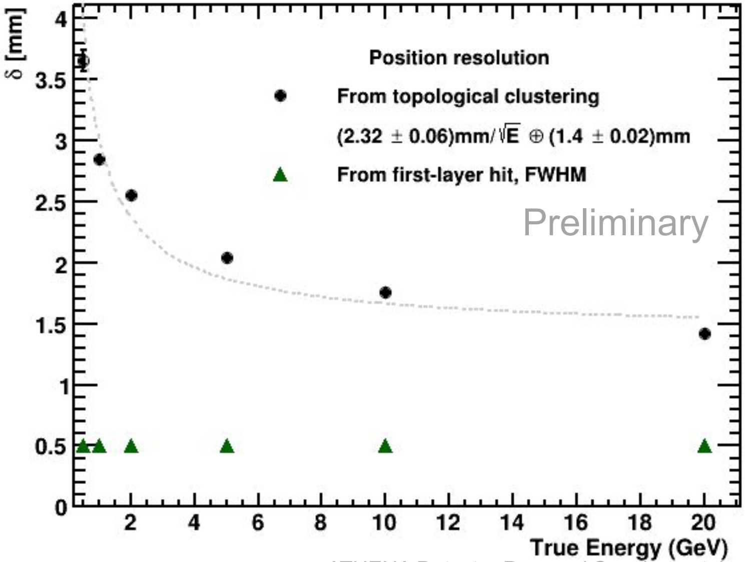

ATHENA Detector Proposal Supplemental material

e/π particle identification

Pion Contamination in Inclusive DIS Physics

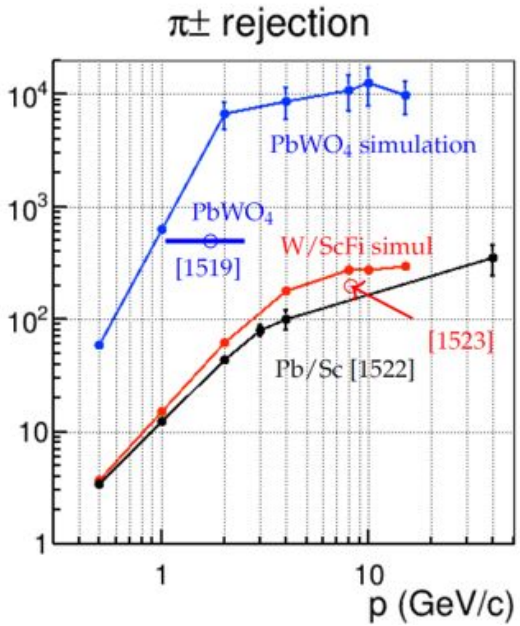

pion:electron > 10^3:1 for p < 2 GeV/c in barrel
No existing calorimetry fully satisfy the requirement

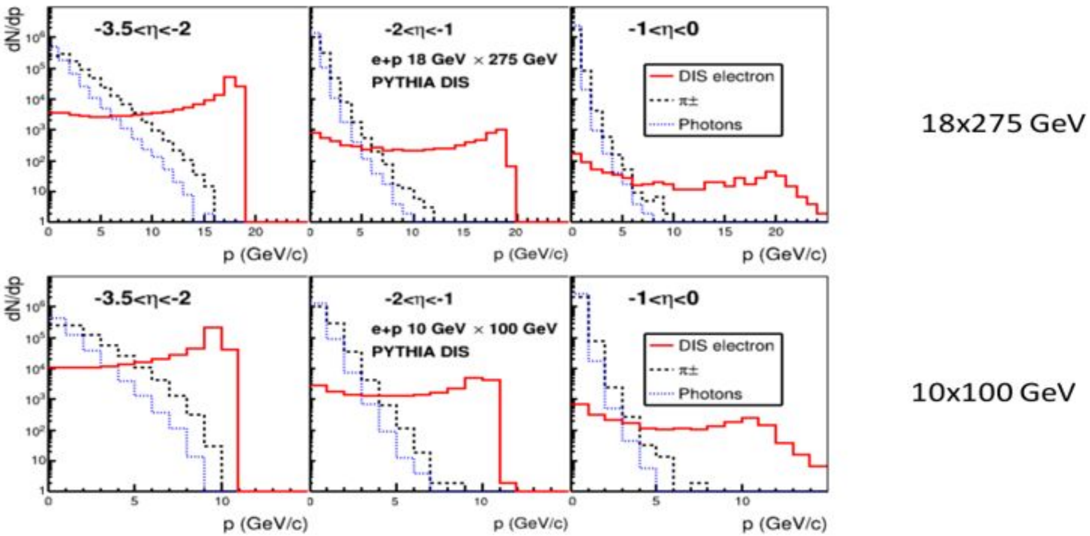

EIC Yellow Report, arXiv:2103.05419 [physics.ins-det]

Two-step Pion Rejection with BECal

Boosting e/pi separation on top of E/p cut with 3D-imaging of particle showers

1: Edep/p cut

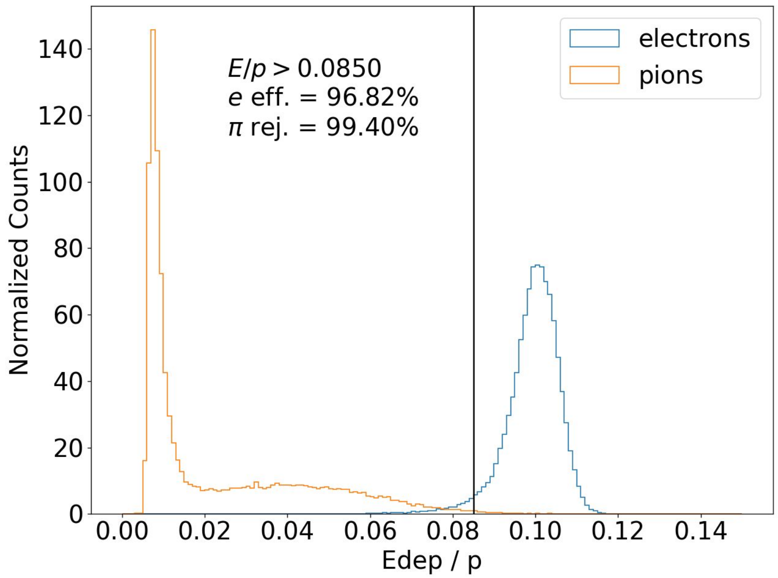

2: NN Classification + Likelihood cut

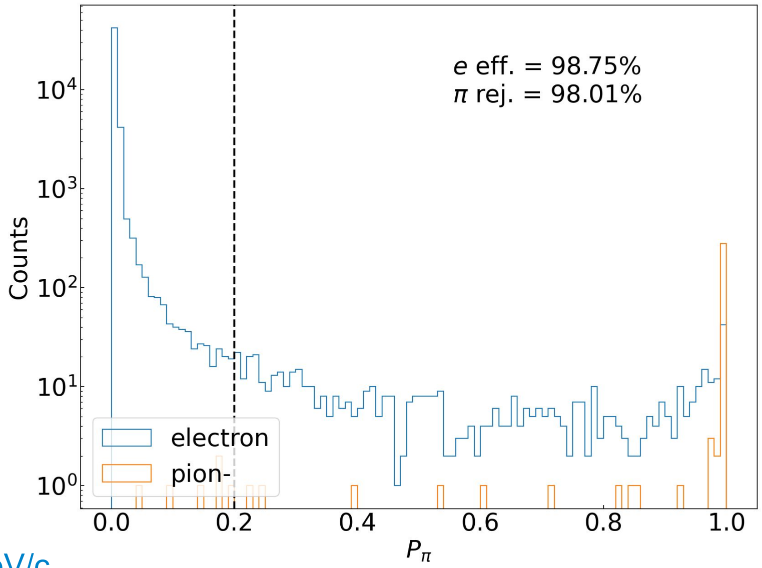

2 GeV/c

Classification Neural Network

- 3 Layers Convolutional Neural Network + 3 Layers Perceptron Network
    - Combined data from AstroPix and Pb/ScFi
    - 3 inserted dropout layers to control overfitting
    - Data formatted to N_events x N_layers x N_hits x N_features
    - 4 features (Edep, Rc, eta, phi), energy and spatial information for shower
    - 125k trainable parameters

- Supervised training
    - 100k events (electrons and pions), 80% training, 20% validating
    - 100k electrons and 100k pions benchmarking
    - 20 epochs
    - Statistical uncertainty (binomial dist.) of benchmarking samples is shown

ELECTRON IDENTIFICATION

$e - \pi$ separation

- Separation of electrons from background π in Deep Inelastic Scattering (DIS) processes

- Best e/pi separation for p < 2 GeV/c
- Comparable to crystal calorimeter at higher momentum
- A factor of 30~100 boost on top of E/p cut for p > 1 GeV/c
- 500:1 rejection at lower momentum from when E/p does not work well

Pion-electron rejection efficiency

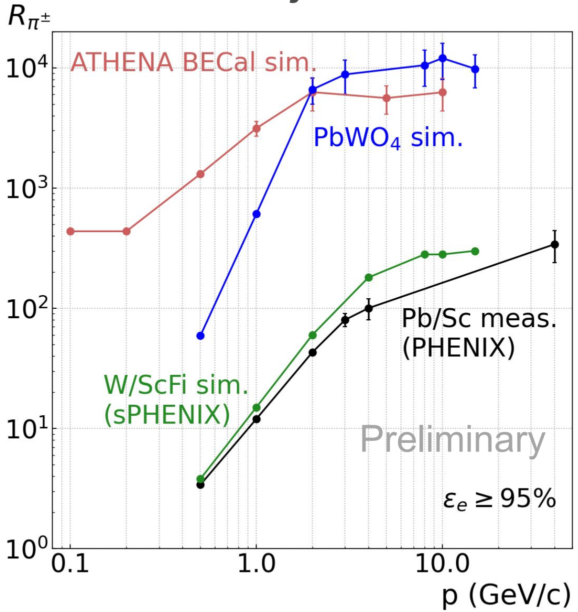

Standalone Calorimeter (no material/no magnetic field)

ATHENA Detector Proposal Supplemental material

Other calorimeter technologies from EIC Yellow Report

Effects from Magnetic Field and Materials

Effect of **3T Magnetic Field** and **material budget in ATHENA Geometry**

- Electron efficiency > 95% for "Standalone" and "w/ MF" simulations

- Electron efficiency is 82% to 92% for "w/ MF and Mat." simulation

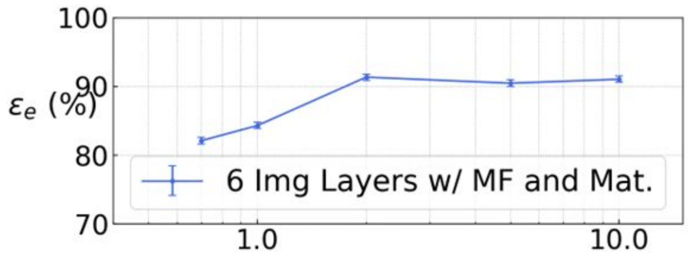

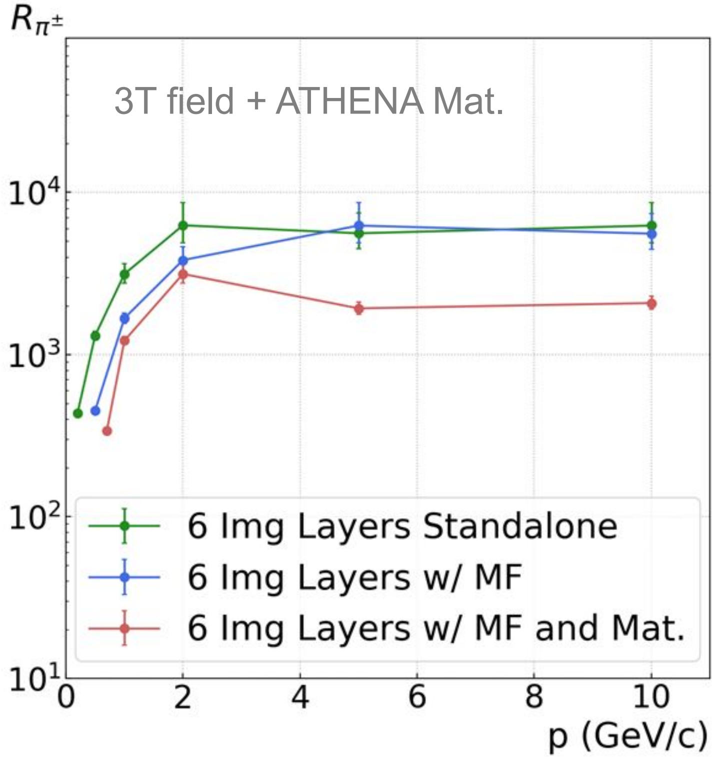

Effects from Magnetic Field and Materials

Effect of **3T Magnetic Field** and **material budget in ATHENA Geometry**

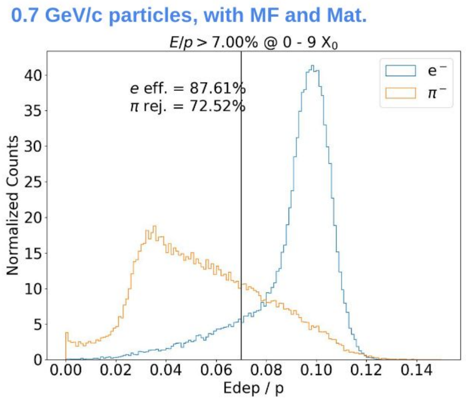

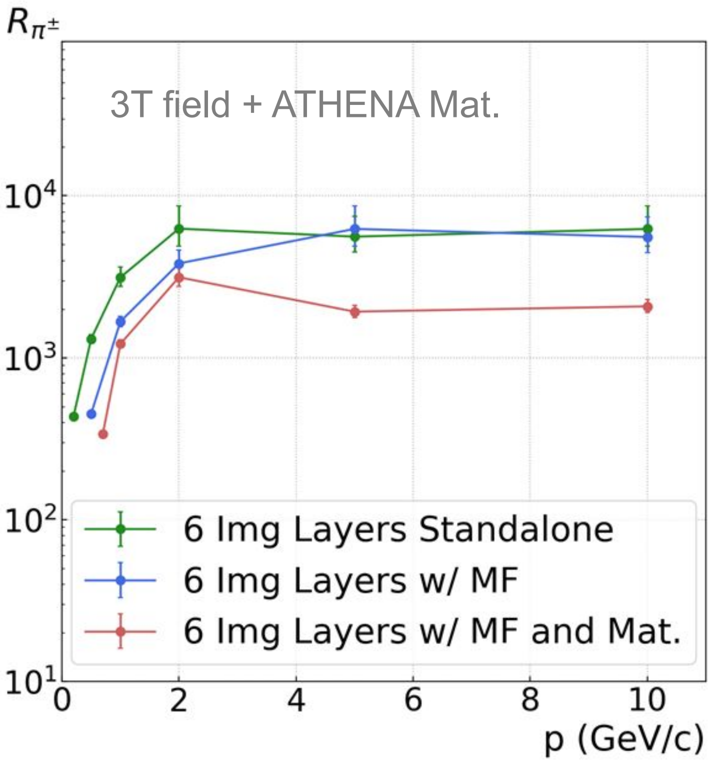

The lowest momentum point for electrons at 0.7 GeV is significantly affected by the high magnetic field.

- The rejection factor will go up with lower field.

Effects from Electron Efficiency

3T Magnetic Field and **material budget in ATHENA Geometry**

- Simulation with magnetic field and materials
- Two extreme cases added
  - > 95% efficiency
  - > 65% efficiency

The lowest momentum point for electrons at 0.7 GeV is significantly affected by the high magnetic field.

- The rejection factor will go up with lower field.

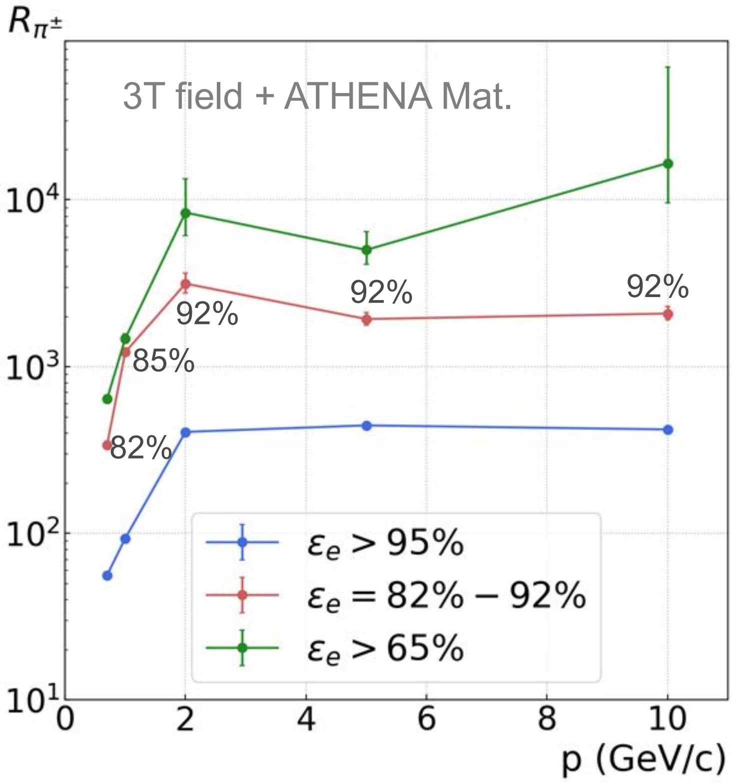

Separation of γ and $\pi^0 \to \gamma\gamma$

Detection of $\pi^0 \rightarrow \gamma\gamma$

EIC Yellow Report, arXiv:2103.05419 [physics.ins-det]

DVCS photons

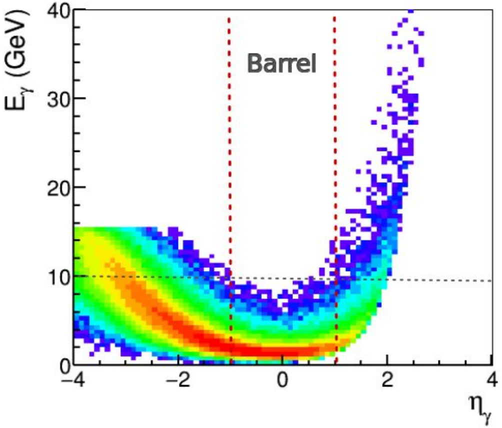

Energy of photons from DVCS versus η from the MILOU simulations for the e+p collisions at beam energies of 18×275 GeV

SIDIS π^0

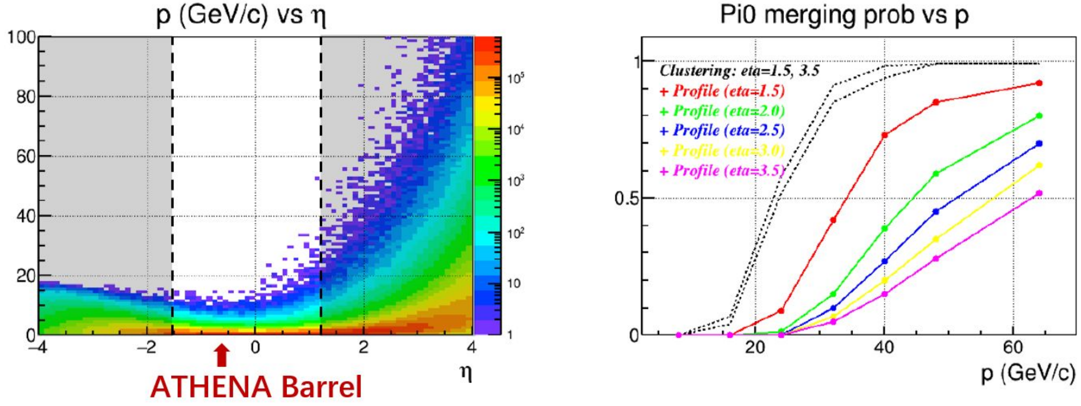

Figure 11.46: Left: The calculated π^0 momentum spectrum for SiDIS at $e + p$ 18 × 275 GeV collisions, using PYTHIA [1371]. **Right**: The probability of two photons to merge, calculated [1517] using GEANT4 [1412] for the cell size of 25 × 25 mm^2 located at 3 m from the interaction point, for the non-projective geometry. For the projective geometry the results for $\eta > 3.5$ would be close to the non-projective curve at for η=3.5.

Hard Limit for Cluster Merging

- For **modular calorimeters**, cell size is the limit
  - No reliable splitting for hits in neighboring cells or the same cell
- For **pixel sensors**, the shower profile is used at different depths

Shower profile from img layers for 5 GeV γs

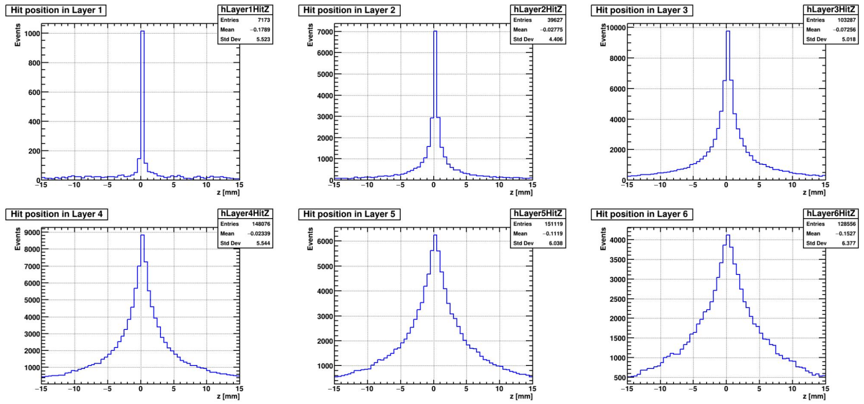

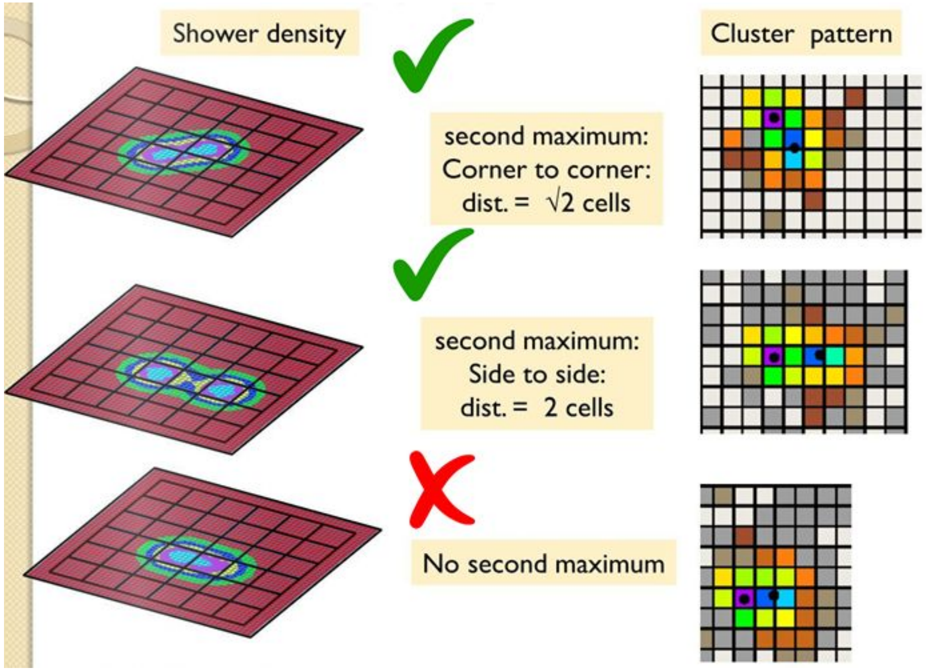

I. Larin, HyCal Clustering

Detection of $\pi^0 \rightarrow \gamma\gamma$

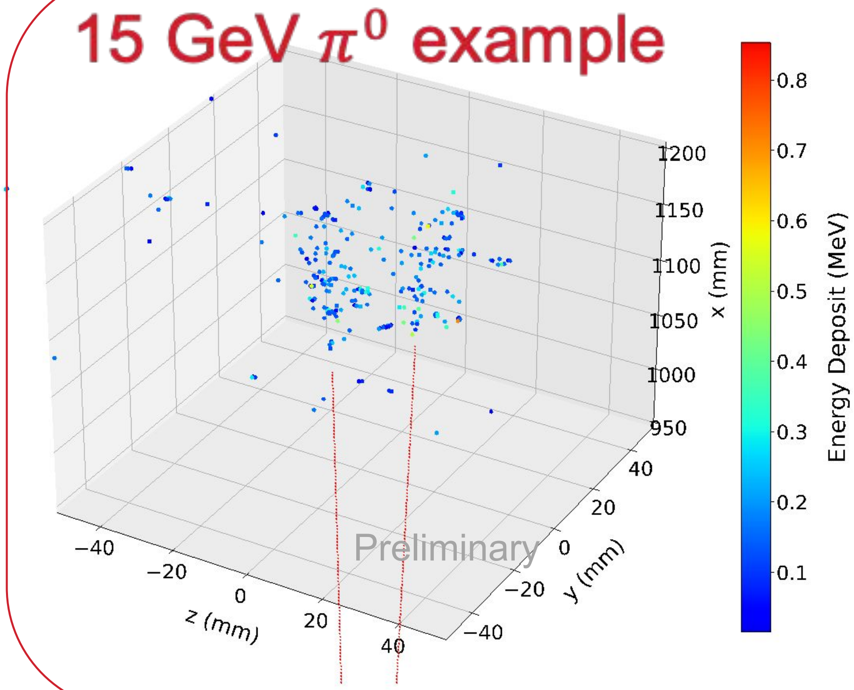

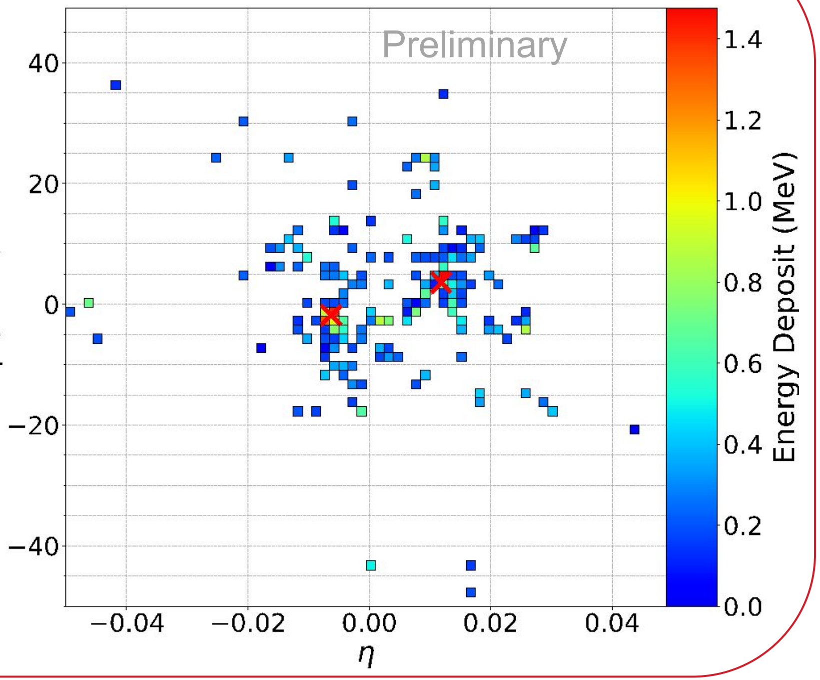

Merging probability for $\pi^0 \rightarrow \gamma\gamma$

π^0 decays in barrel region

Detection of photons at **R = 1.03 m**

Cut out-of-acceptance events

Cut very low energy events
(photons with energy > 100 MeV used)

Hard limit of merging

- Cell size for modular calo
- For AstroPix: 6 FWHM of shower profile at the layer where at least 90% of gammas fired a hit

Used shower profile (6FWHM)

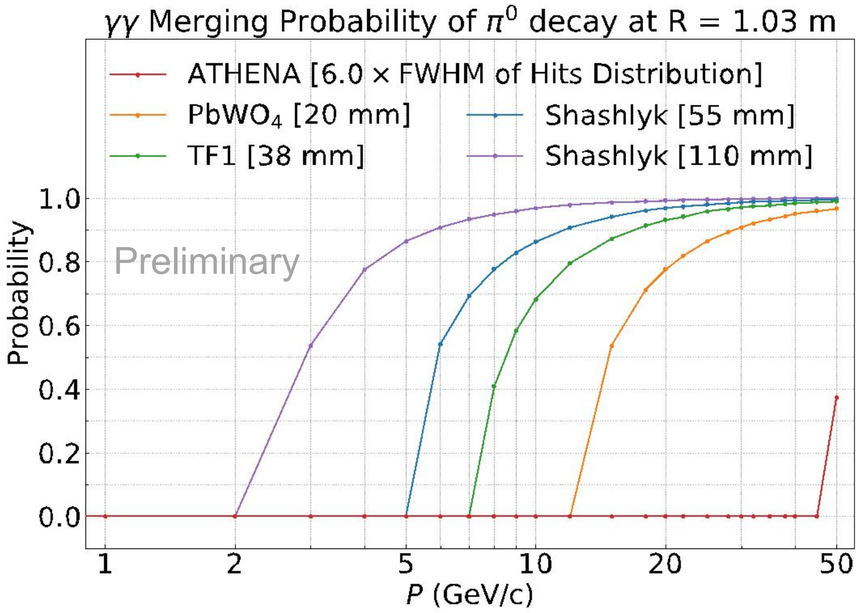

ATHENA Detector Proposal Supplemental material

Merging probability for $\pi^0 \rightarrow \gamma\gamma$

π^0 decays in barrel region

Detection of photons at **R = 0.8 m**

Cut out-of-acceptance events

Cut very low energy events
(photons with energy > 100 MeV used)

Hard limit of merging
- Cell size for modular calo
- For AstroPix: 6 FWHM of shower profile at the layer where at least 90% of gammas fired a hit

Used shower profile (6FWHM)

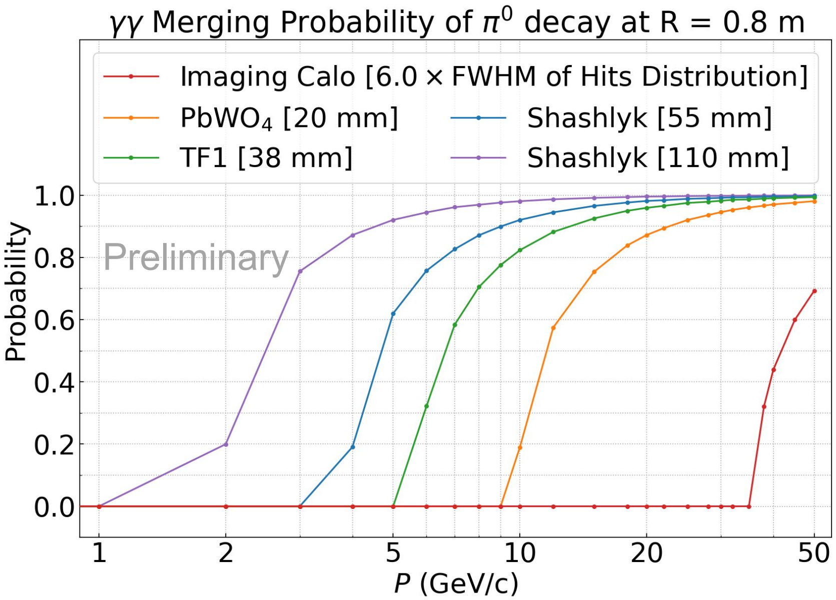

Note! Shower profile from ATHENA simulation w/ 3T field. Just a first check at r = 80 cm.

Particle PID

MUONS IN BARREL

for 3T field

- Muon/pion separation in **central region** determined from information from the **Barrel ECal** and **HCal**
- Results for single particle simulation, **see details in the following slides**

π contamination

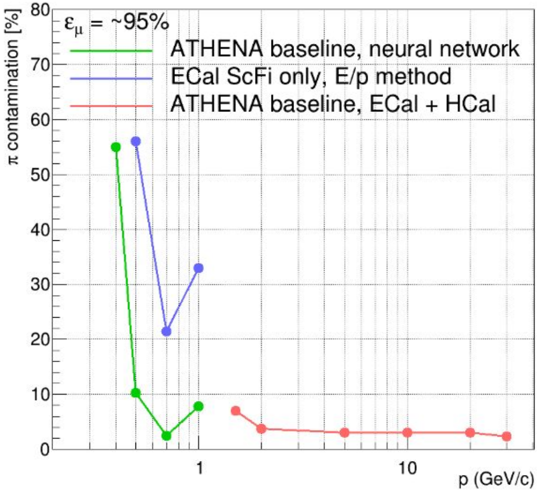

μ efficiency

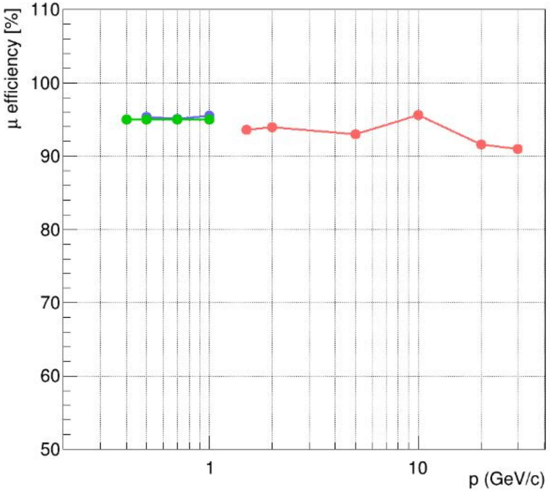

- **At η = 0: muons >~1.5 GeV/c reach HCal, and <~1.5 GeV/c curl inside the BCal** (different approach to analysis)
  - ➢ This discontinuity (in reaching HCal) is rapidity dependent
- Neural Network studies in ECal done for η = (-1,1), ECal+HCal studies and E/p studies in ECal done for η = 0
- Further improvements to muon/pion separation from PID detectors expected (DIRC)

SUMMARY AND OUTLOOK

1. Hybrid Imaging ECAL calorimeter proposed for the future Electron-Ion Collider
   – Scintillating fibers embedded in Pb and imaging calorimetry based on silicon sensors (AstroPix)

2. Novel technology, yet with limited risk

3. This, cost-effective for its excellent performance, design fulfills and further improves the Yellow Report requirements and opens new physics opportunities:
   – Excellent Energy and Spatial resolution
   – Electron-pion separation at low particle-momenta
   – Separation of two gammas from neutral pion up to 45 GeV
   – Muon PID, radiative processes, …
   – Can serve as DIRC tracking layer and inner HCAL

Backup

GlueX Energy Resolution

The resolution 5.2%/√E ⊕ 3.6% is for the typical momentum range for pi0 and eta in GlueX and integrated over typical angular distributions for pi0 and eta production (0.5-2.5 GeV).

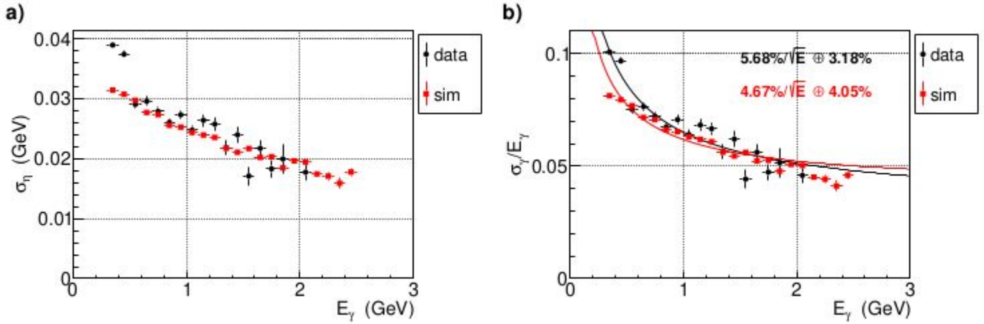

Figure 32: a) Measured and simulated η width as a function of energy for symmetric decays, where both photons are required to be within 0.1 GeV of each other. b) The energy resolution of single photons calculated under the assumption that only the energy resolution contributes to the η width. The curves are fits based on Eq. 4 (Color online)

We note that the response of the calorimeter averaged over its length, as done for the η sample in Fig. 32, is not described well with Eq. 4 and ***has a large correlation between the two parameters (-0.89)****. Nevertheless, in order to characterize the performance of the BCAL between 0.5 and 2.5 GeV, we take the fitted energy-resolution parameters integrated over the angular distributions for π0 and η production to obtain a typical energy resolution for our detector of 5.2%/√E ⊕3.6%. In order to estimate the resolution at high energy, we use the MC that describes our data at low energy (Fig. 33) and results in a constant term of* ***less than 1.7%****. However, to verify this expectation, we would need additional data reaching to higher energy.*

GlueX Energy resolution

GlueX Calorimeter is 15.3 X0 thick at normal angle

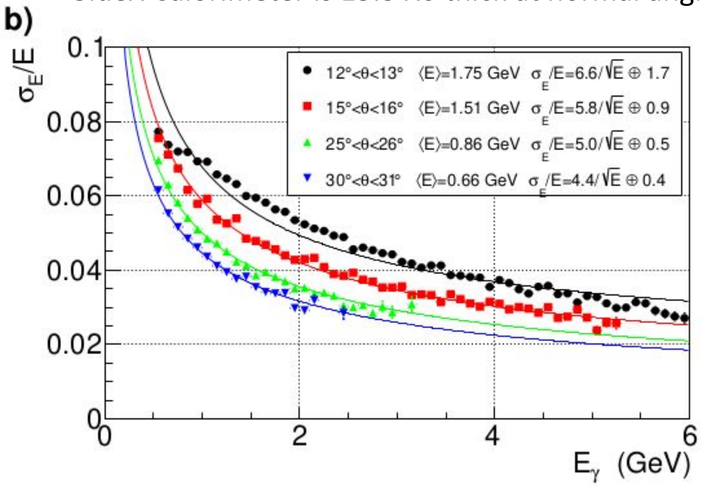

Figure 33: Simulated fractional energy resolution for data at different angles from the target for the distribution in Fig. 31a. At shallow angles the stochastic term increases and the energy leakage generates a non-zero constant term. The MC data points are fitted to Eq. 4 with the results shown in the legend. (Color online)

e/π particle identification

Performance Impact

- Electron/Pion Separation
  - Imaging layers significantly improve electron/pion separation

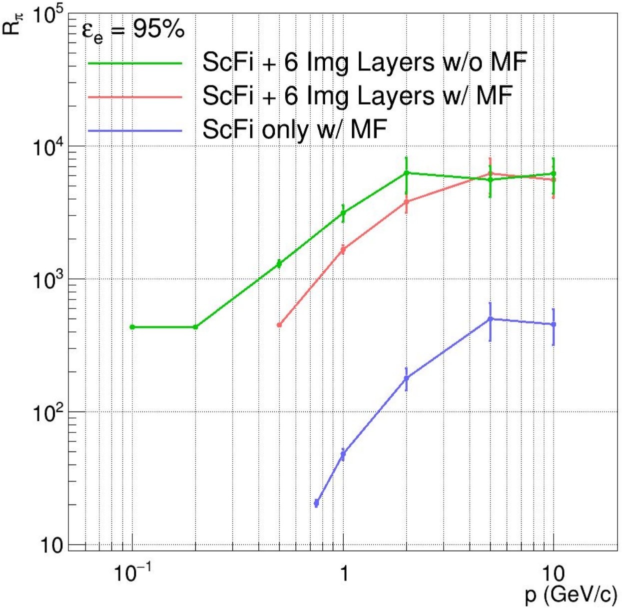

With ScFi only: pion suppression based on E/p cut utilizing sum of deposited energy at different calorimeter depth

With imaging layers: order of magnitude improvement in pion suppression with ML methods utilizing 3D spatial and energy information of the shower profile

Yellow Report requirement: R_π up to 10^4

Performance Impact

- Full geometry of ATHENA
  - Materials from other PID detectors inside barrel
  - Efficiency for electron drops to ~91%

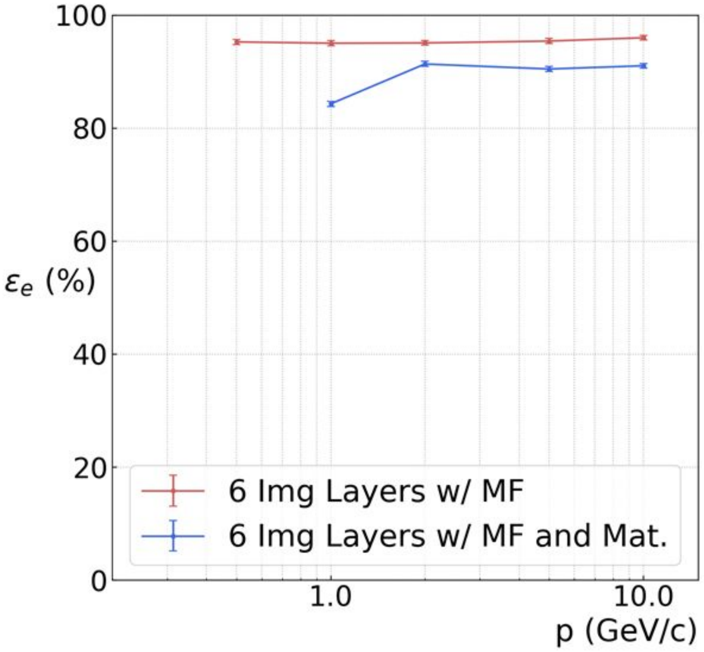

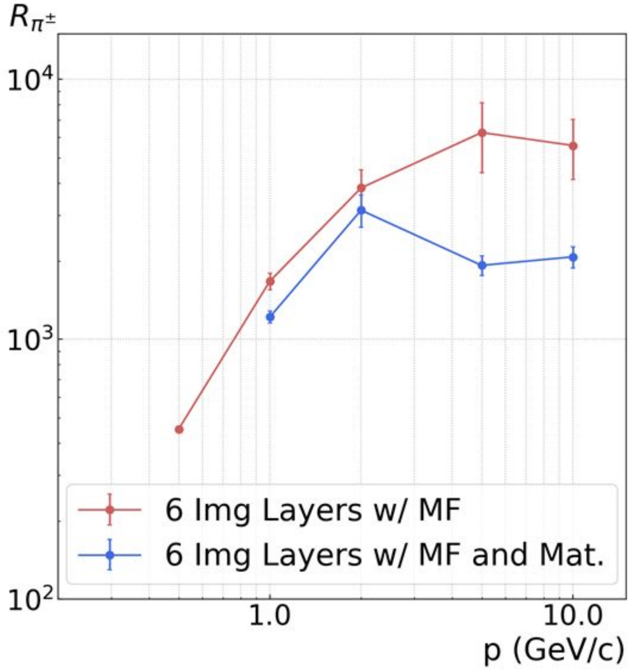

Pion Rejection Power

Solid line: 6 AstroPix Layers
Dashed line: 9 AstroPix Layers

- Best e/pi separation for p < 2 GeV/c
- Comparable to crystal calorimeter at higher momentum
- A factor of 30~100 boost on top of E/p cut for p > 1 GeV/c
- 500:1 rejection at lower momentum from when E/p does not work well

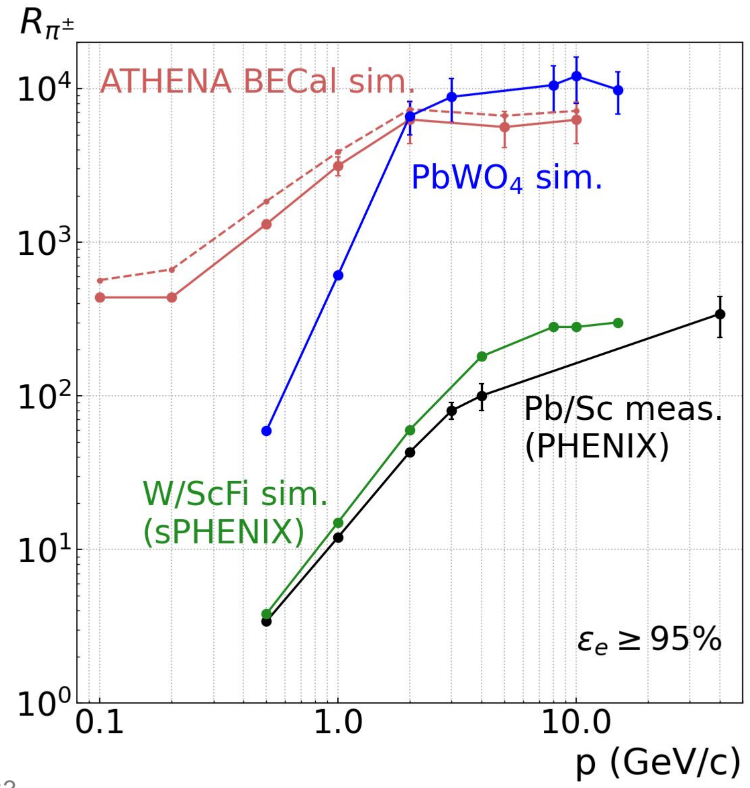

Number of imaging layers

3D shower imaging:

- **3 layers** at the beginning of the shower development to capture the **signals of the shower/preshower starting point** for most of the electrons and photons.
  - Photons may shower at greater depth, the study of photon shower hits distribution shows this
  - Important for photon physics for the position resolution and π/γ separation based on shower profile

- **2 layers** needed **to sample the most dense part** of the shower development
  - Important for e/π shower shape separation, particle PID
  - Important for full 3D cluster reconstruction. Full 3D cluster reconstruction is affected by small number of hits (visible for low energy particles).
  - 3D cluster reconstruction important for spatial resolution for photons.

- **1 layer** needed **for the shower tail**
  - Important for e/π shower shape separation, particle PID (hadrons, muons)

First img layer that photons leave a hit at

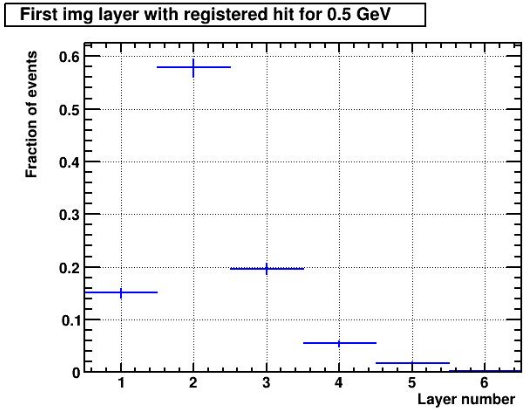

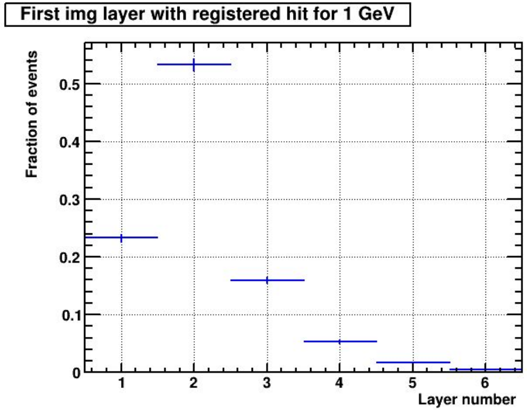

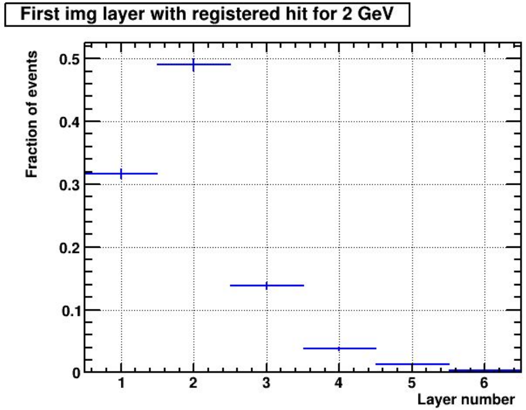

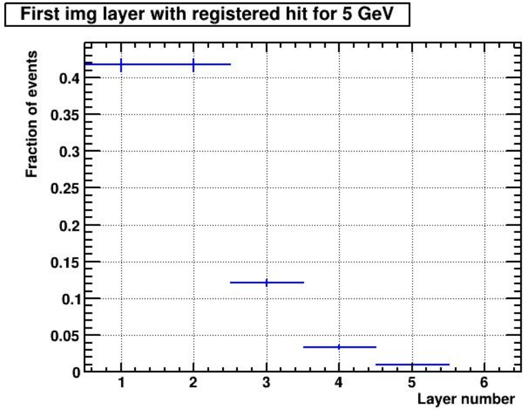

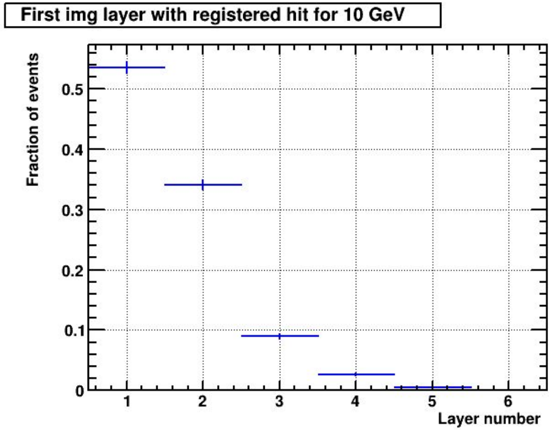

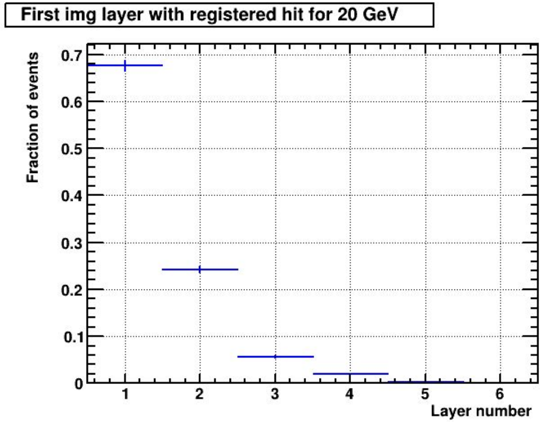

Average number of hits per layer

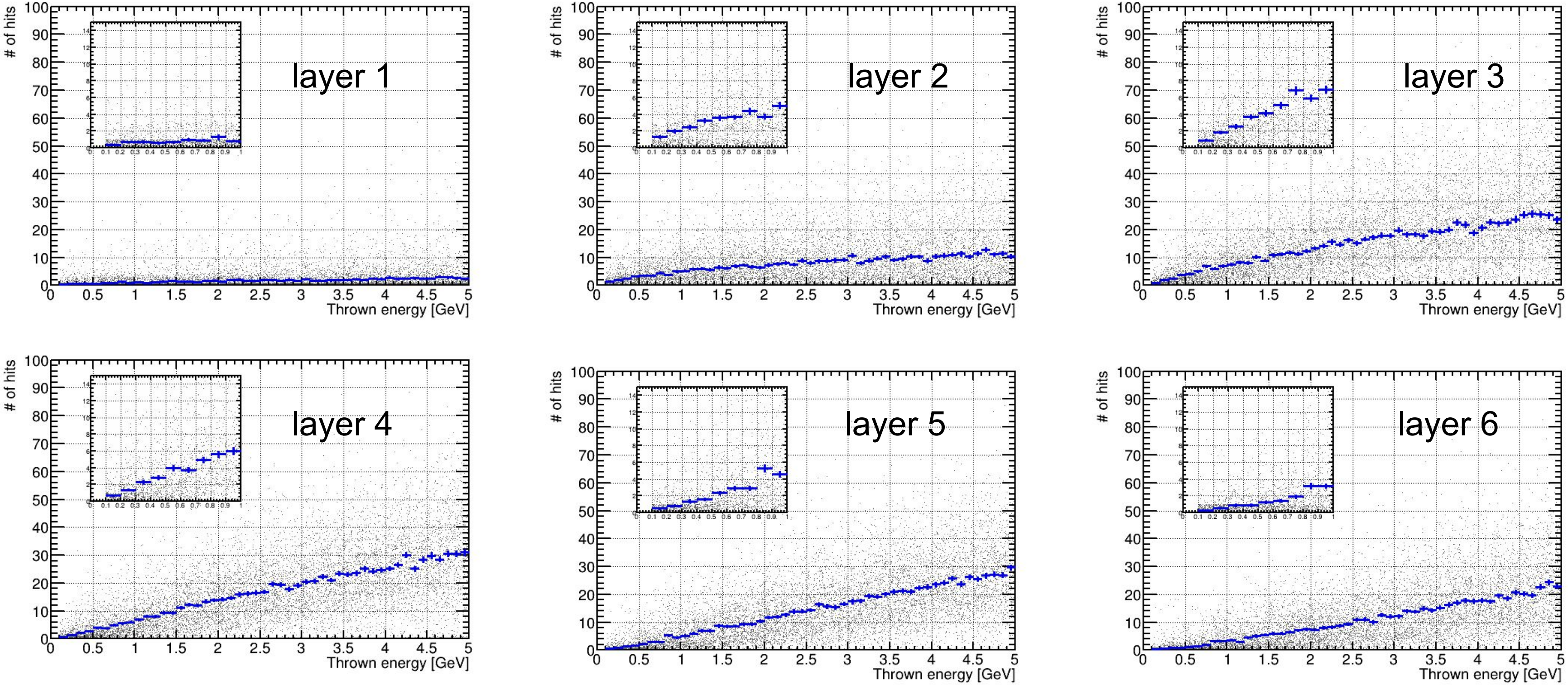

Average number of hits in 6 layers

Number of hits

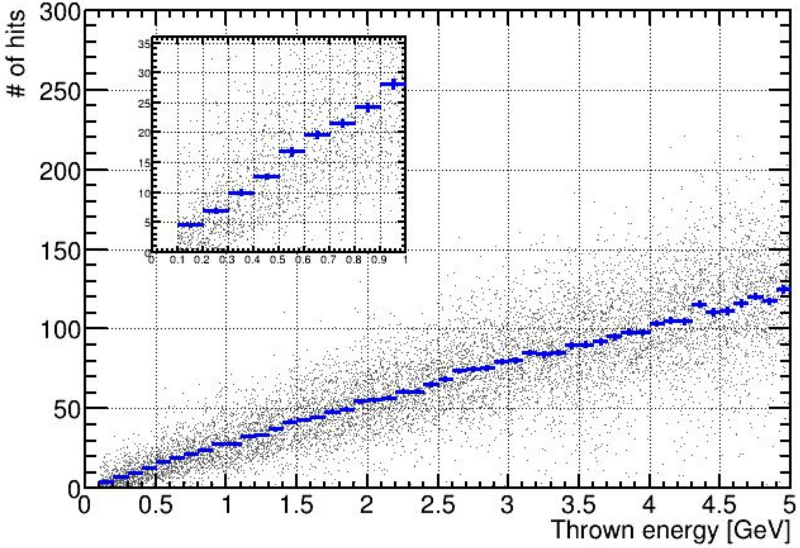

Deposited energy (reconstructed)

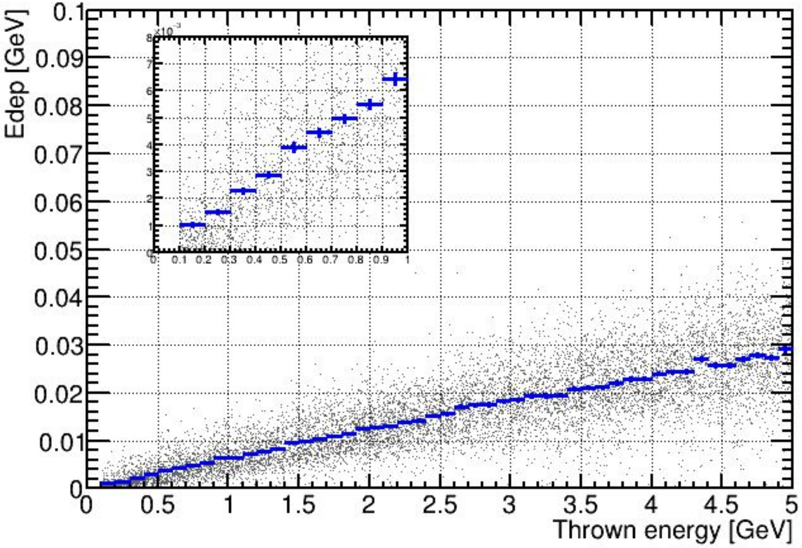

Example of cluster reco optimization

Work in progress
S. Kaur

Nhits = 18 , min edep = 0.5MeV , distXY = 2.5mm

Nhits = 6 , min edep = 0.5MeV , distXY = 2.5mm

Photons

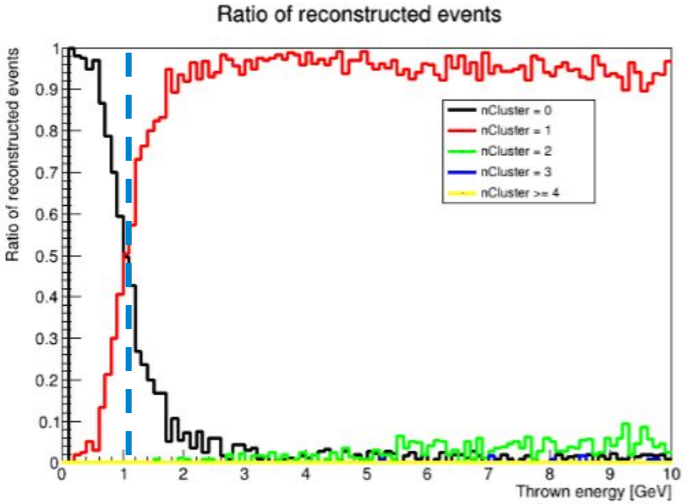

Initial optimization for high E photons > ~1 GeV

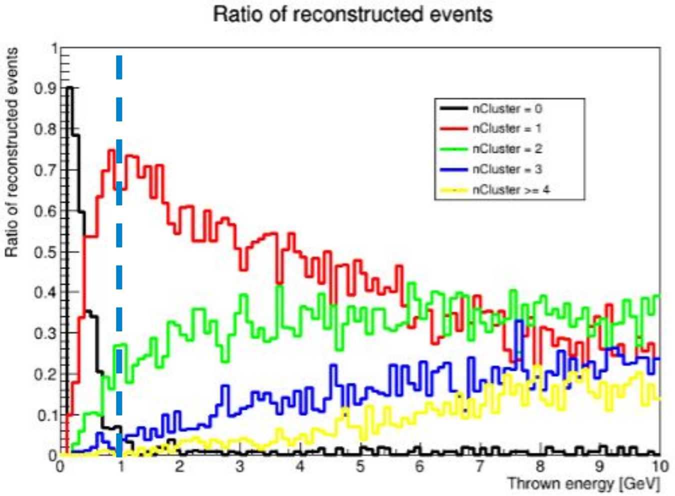

Initial optimization for low E photons < ~1 GeV

~ 50%

Pion Rejection Power - Different Nb of Layers

9 layers → 6 layers
about a factor of 1.5 in pion rejection power

9 layers → 7 layers
similar performance at higher momentum

6 layers → 7 layers
small improvement at lower momentum as compared to

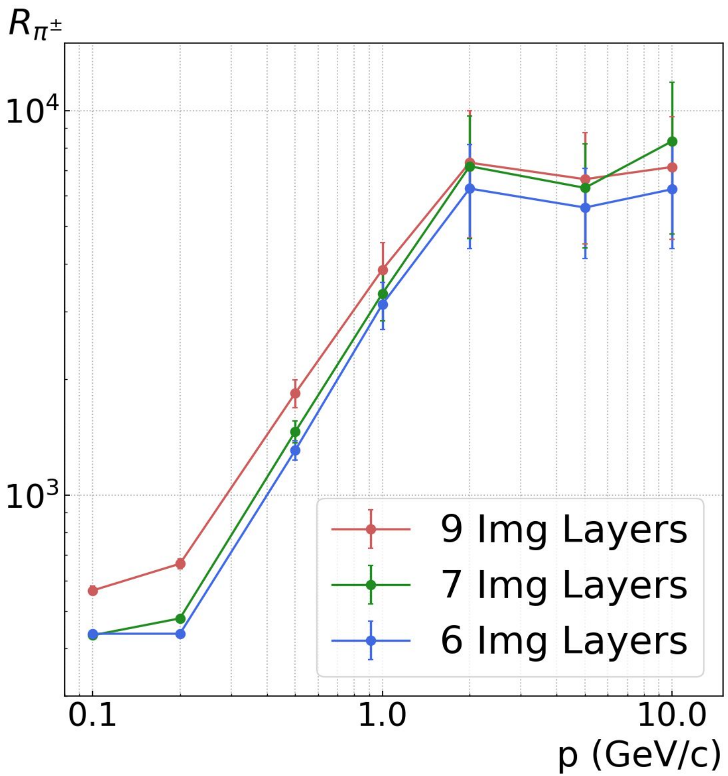

Standalone performance, no material in front, no field

Pion Rejection Power - Different Nb of Layers

- With 5 layers, we will experience a drop of about 20~50% for the rejection power
- Low energy point affected by magnetic field
- Efficiencies as shown below for 6 Img layers

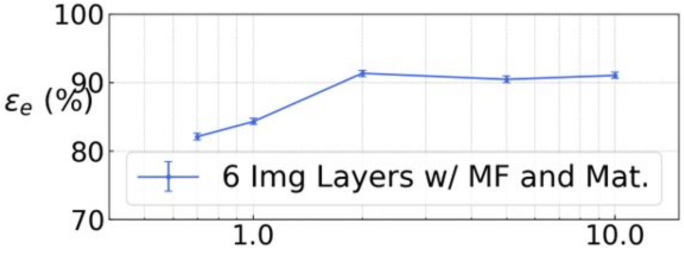

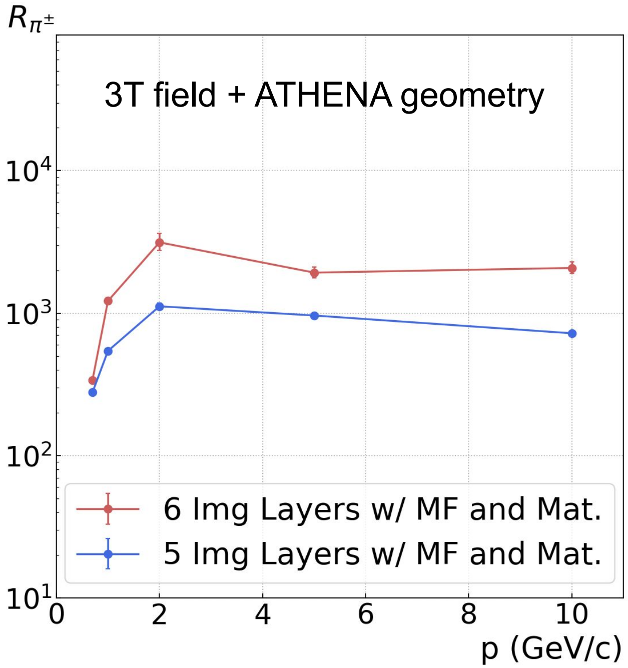

Reconstruction methods

Clustering

Current in juggler analysis framework, the clustering is done by

1. digitization -> simulation hits to readout signals
2. readout reconstruction -> readout signals to energy/timing/position/etc (calibration)
3. proto-clustering -> group hits following certain algorithms
4. cluster reconstruction -> reconstruct position/energy/etc from group of hits

Two clustering algorithms are available now

1. Island clustering for 2D hits
2. Topo clustering for 3D hits

Island Clustering

Group all neighbouring hits

- Parameterized conditions for finding neighbors
- Distance in local-XY, local-XZ, local-YZ,
- local-XY scaled by cell dimensions,
- global eta-phi, global R-phi

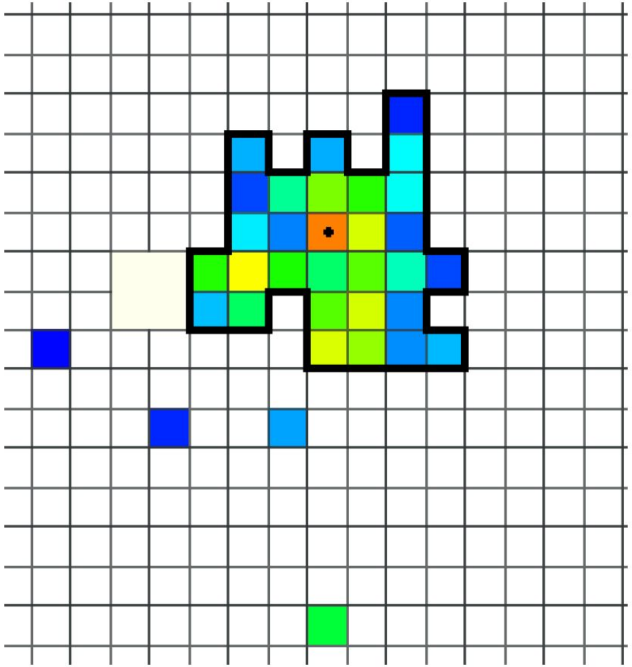

Parameterised minimal energy to be qualified as cluster center, and minimal energy to participate clustering

Island Clustering Splitting

Cluster splitting is available for Island Clustering

- Split based on Local maxima that are qualified as cluster center
- Hits energy split based on local maxima's energies and distances

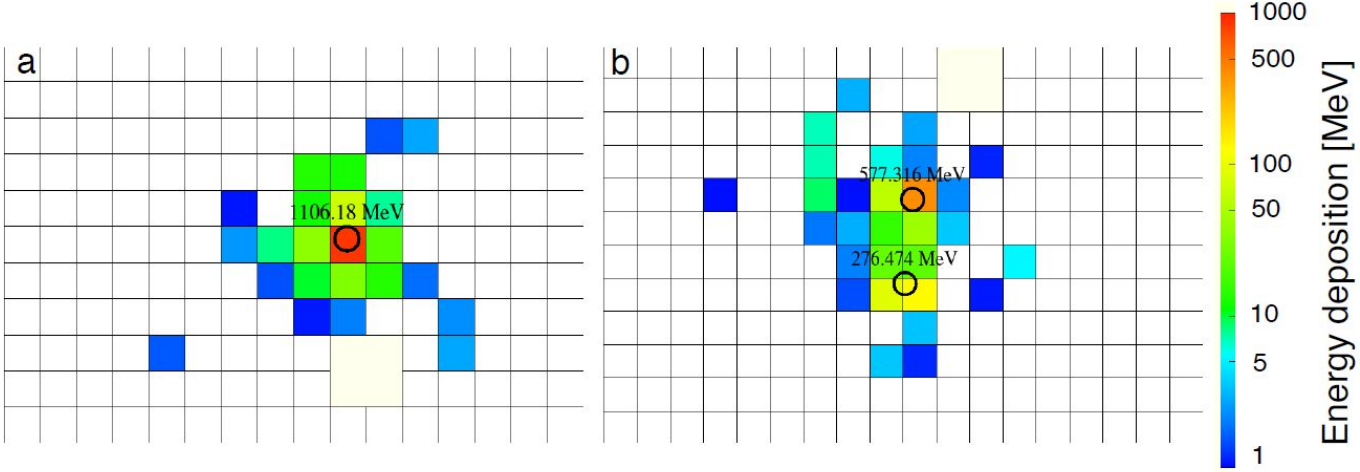

Topo Clustering

Similar to Island clustering but works for hits from several layers, currently used for imaging layers

Hits at the same layer, local-XY

Hits from different layers, layer id difference and global eta-phi

Hits from different sectors, global distance

No splitting implemented currently

- Mostly MIP signals in imaging pixels

3D Clustering Samples

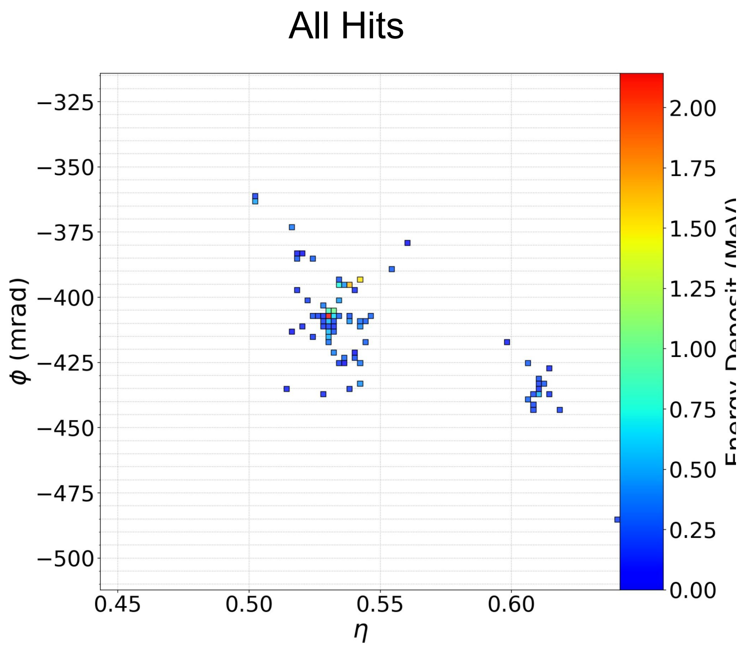

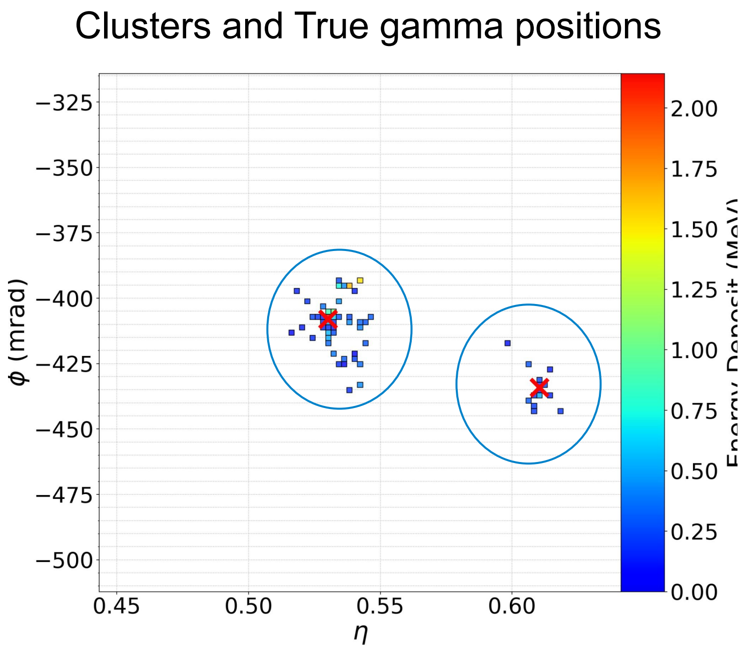

3D Clustering Samples

All Hits

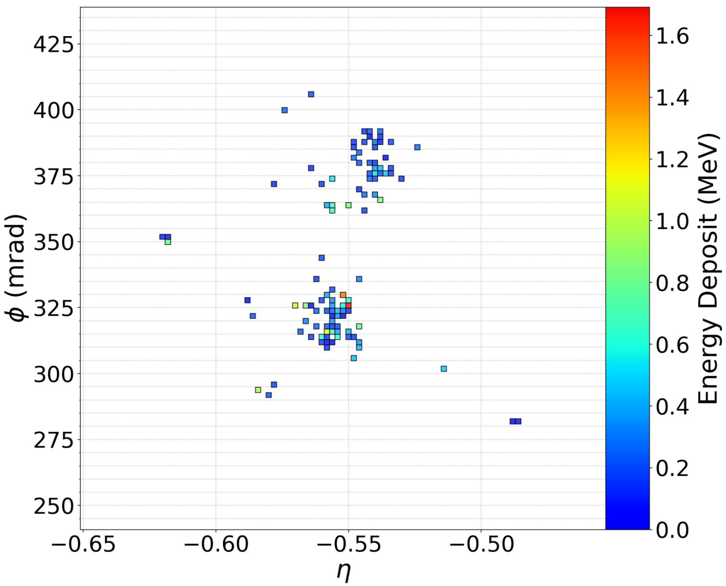

Clusters and True gamma positions

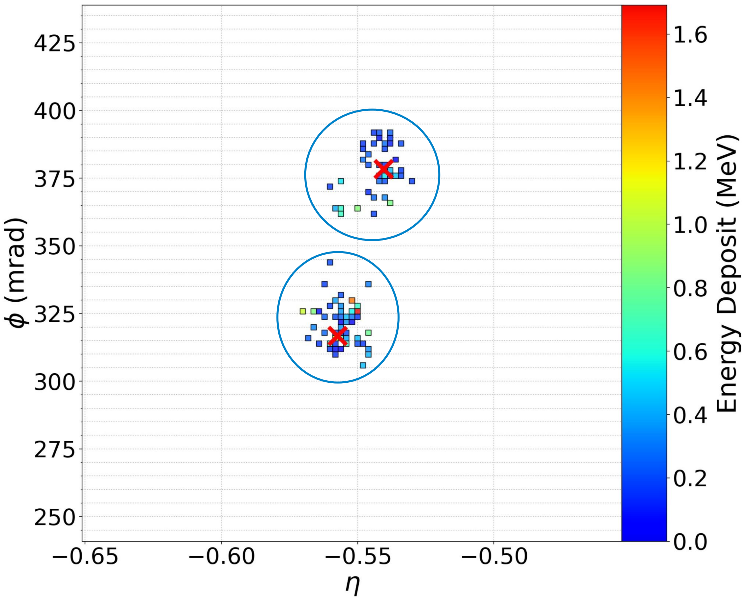

Readout

Dynamic Range

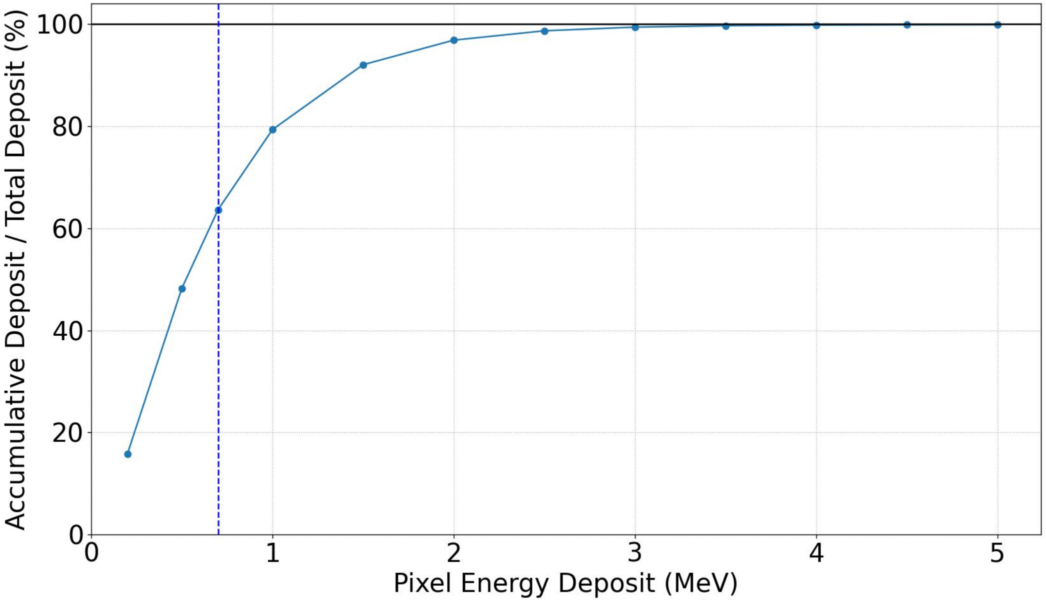

- Dynamic range for AstroPix v1: 700 KeV
- To be extended to a few MeV for the proposed calorimeter
- 3 MeV range will cover over 99% of the deposited energy (2 GeV electron simulation)

Occupancy

- Readout system: **two-levels aggregators**
- Each stave of the detector: **8 first-level aggregators** (~0.3 m^2)
  - collect the signals from the covered area and send the data to the second-level aggregators
- **2nd lever aggregator**: inject the AstroPix layers data into the main data stream; also participate in the trigger forming for the whole ATHENA detector.

Layer Number	Stave Area (m^2)	N_{pix} / Stave	N_{pix} / Aggregator
1	2.24	89k	11k
2	2.30	92k	11k
3	2.36	94k	12k
4	2.42	97k	12k
5	2.48	99k	12k
6	2.54	101k	13k
7	2.60	104k	13k
8	2.66	106k	13k
9	2.72	109k	14k

Occupancy

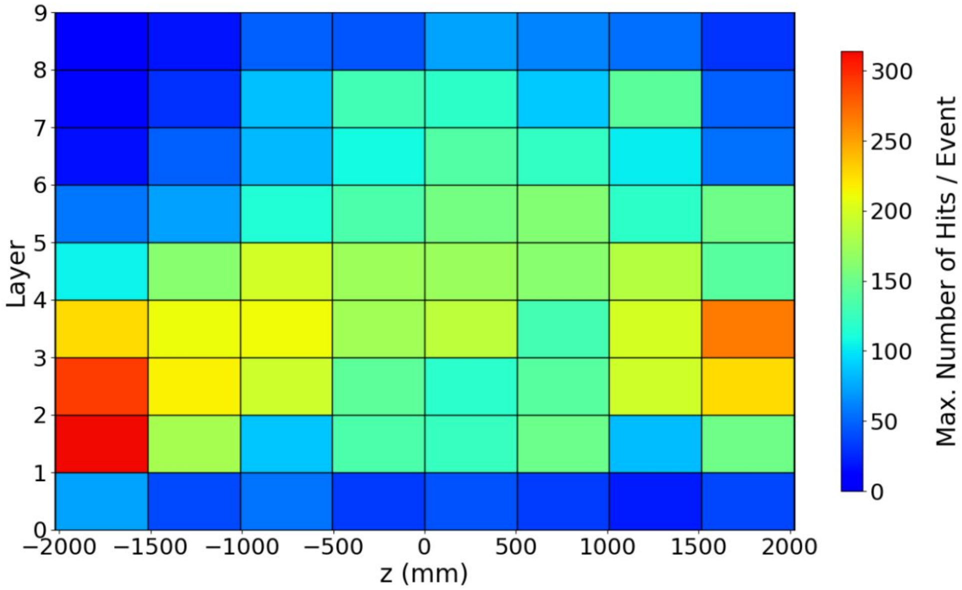

Figure 18: The maximum number of hits in first-level aggregators from single-particle simulation with 20 GeV electrons. The electrons were uniformly generated to scan the whole geometrical acceptance of the barrel calorimeter. One stave of the barrel calorimeter, including 9 AstroPix layers and 8 aggregators per layer, is shown here. Each block in the plot represents an aggregator. The hot regions at both ends are due to geometrical effects caused by endcap calorimeters.

Ionization radiation and neutron flux

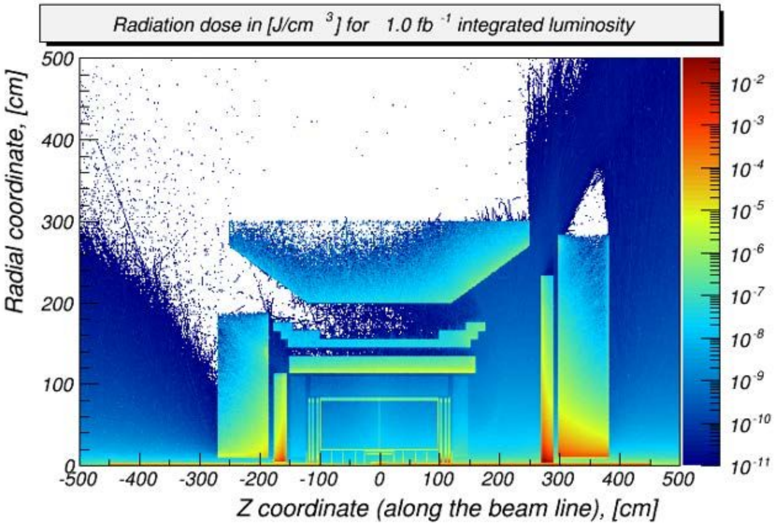

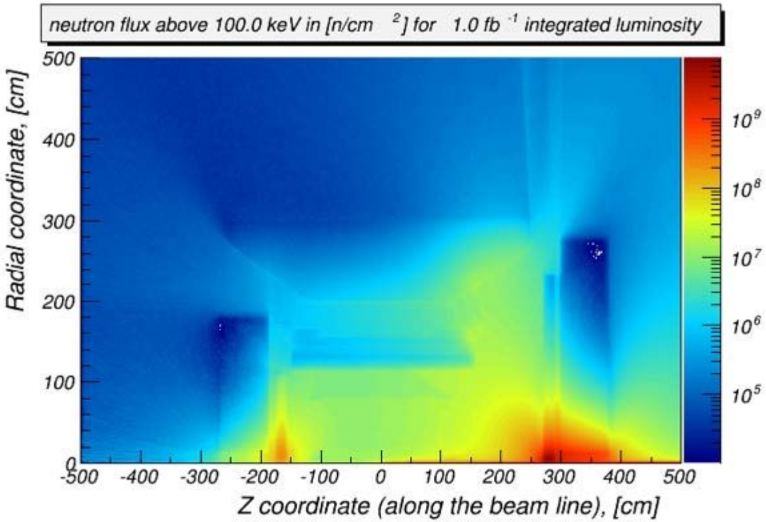

- Maximum ionizing radiation dose from e+p collisions at the highest EIC luminosity ($10^{34}cm^{-2}s^{-1}$): ~1 Rad/year
- Neutron flux: 10^8 neutrons/cm^2 per year at the top luminosity (two order of magnitude lower than the near-beam-line detectors)

Reconstruction of π^0

2 GeV photons, y position

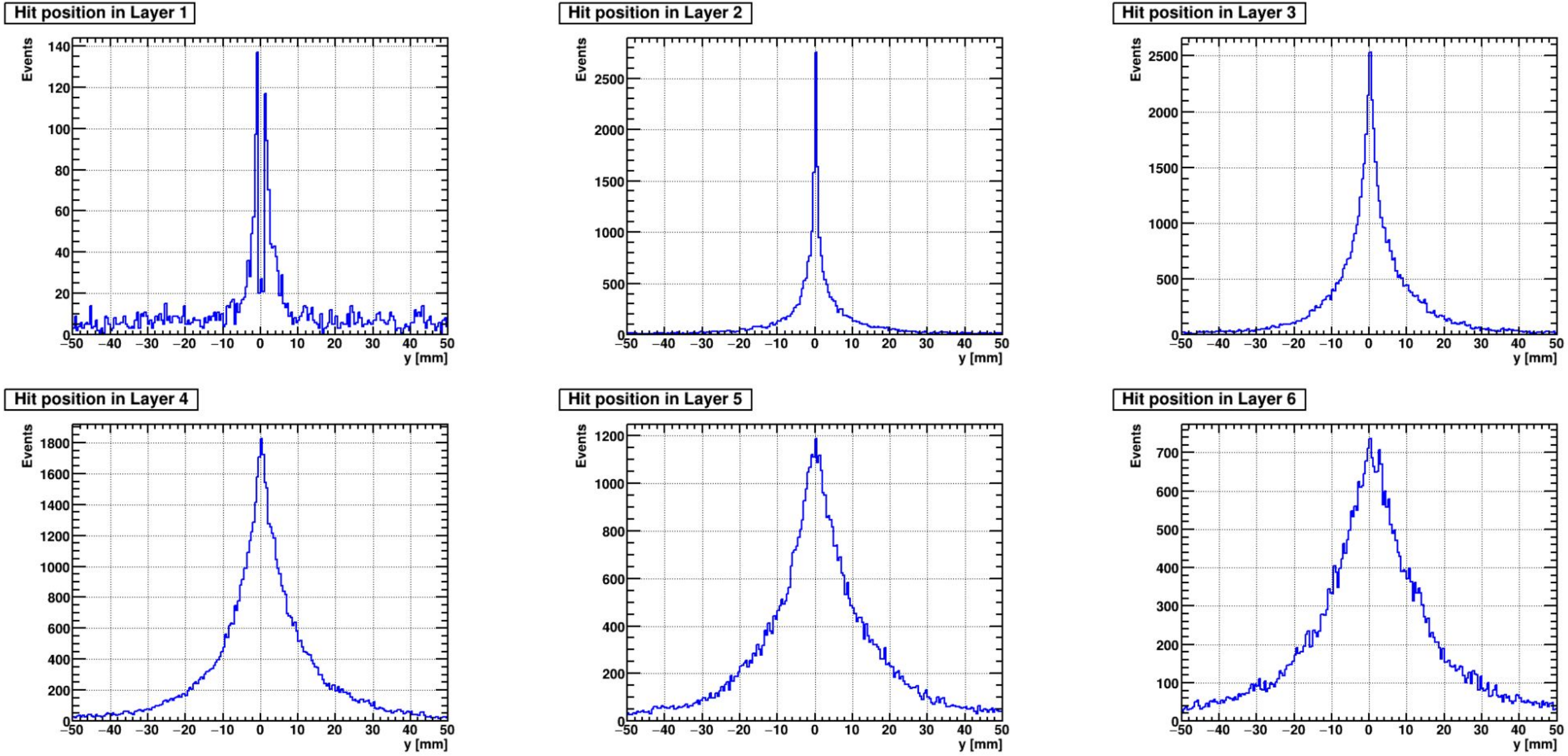

2 GeV photons, z position

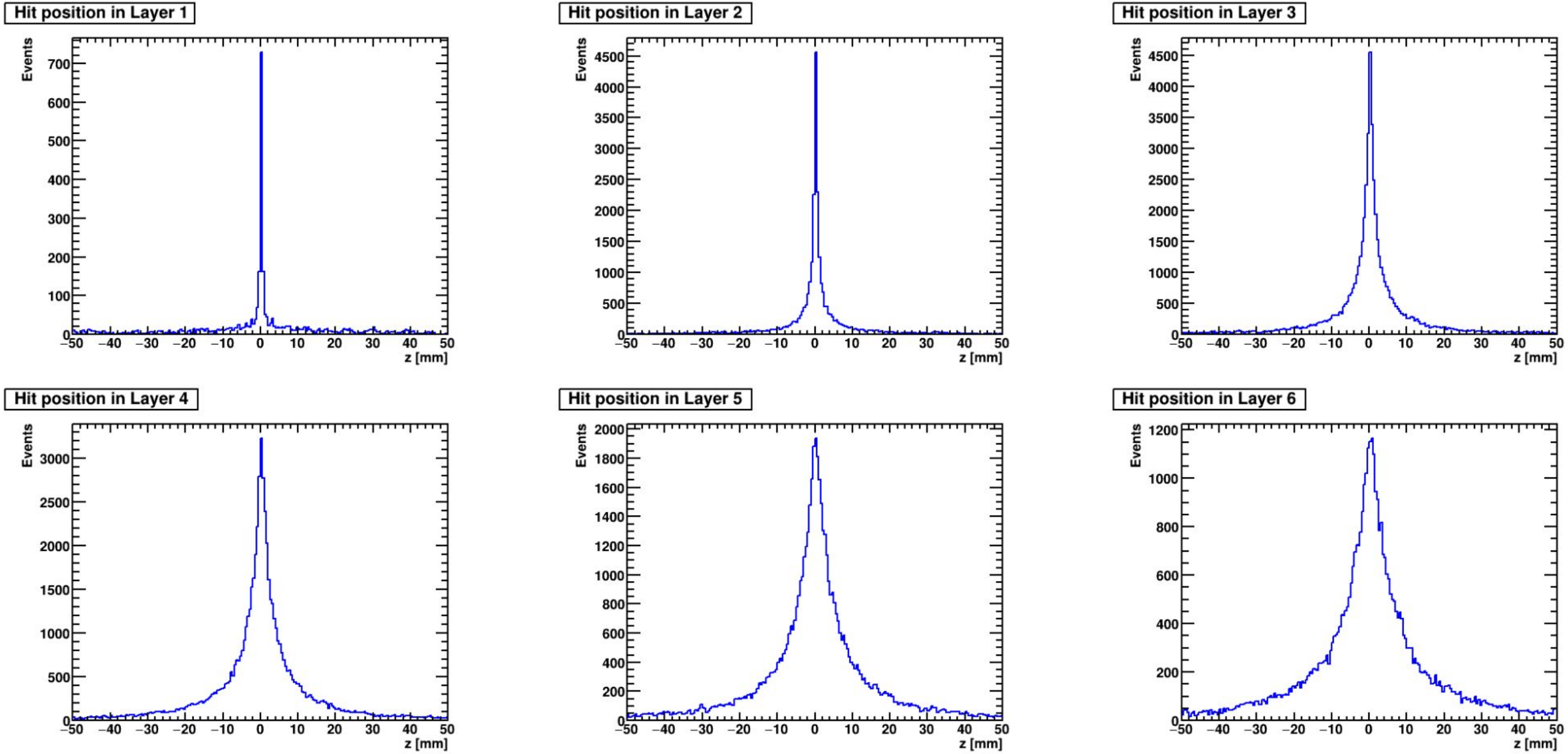

FWHM of shower for layer 1, 2, and 3

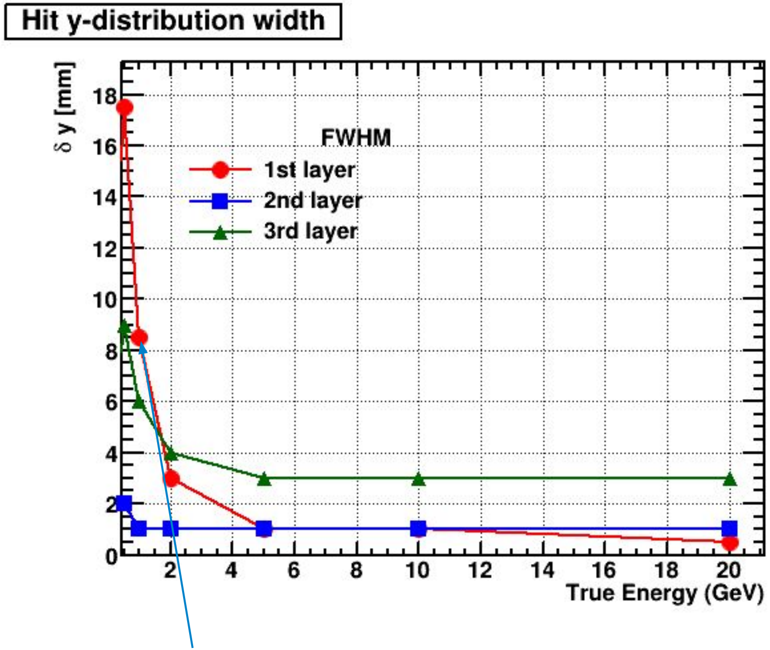

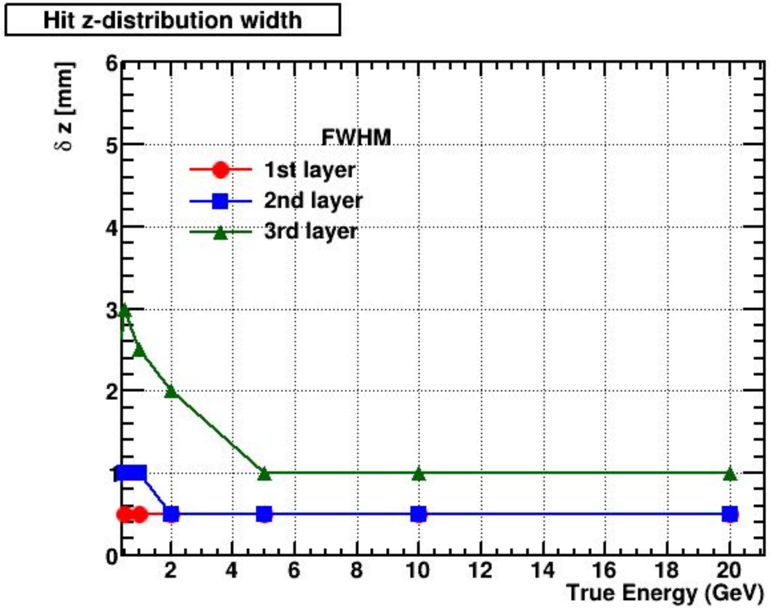

For low energy (0.5, 1, 2 GeV) in 1st layer we see double-peak in y distribution (e+e- from interaction before calorimeter). FWHM reflects the width of the whole hit position distribution here, not individual peaks.

FWHM of shower for layer 1, 2, and 3

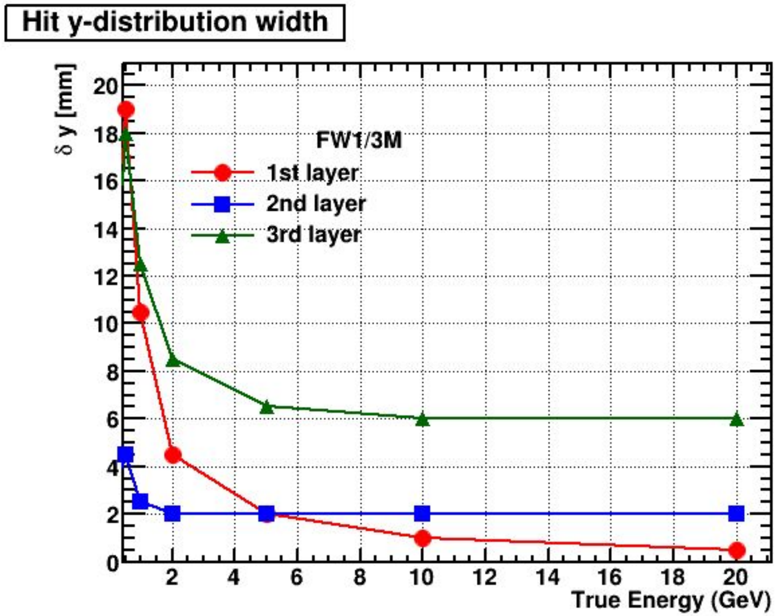

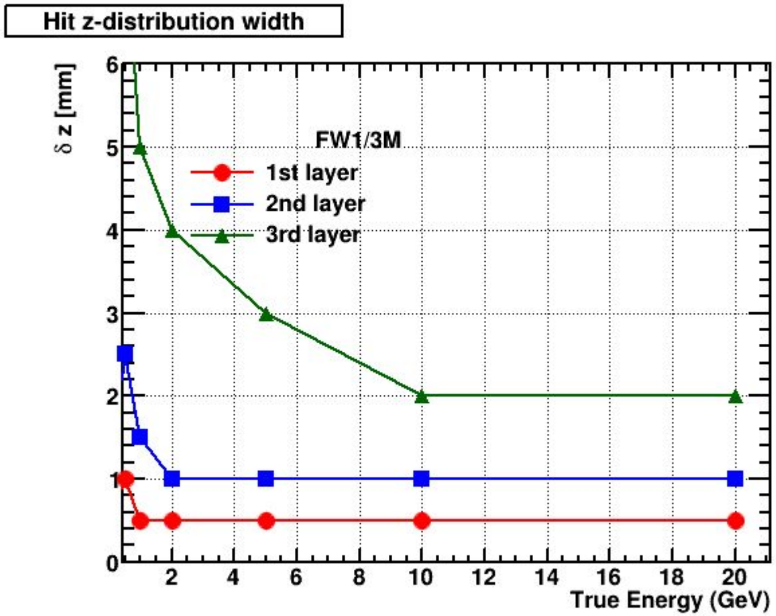

For low energy (0.5, 1, 2 GeV) in 1st layer we see double-peak in y distribution (e+e- from interaction before calorimeter)

First img layer that photons leave a hit at

First img layer with registered hit for 0.5 GeV

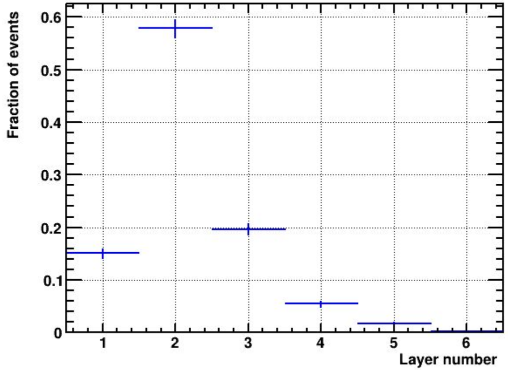

First img layer with registered hit for 1 GeV

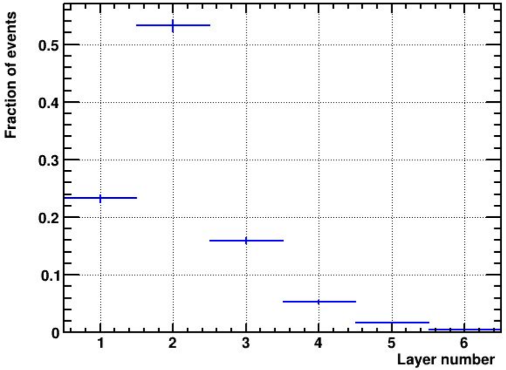

First img layer with registered hit for 2 GeV

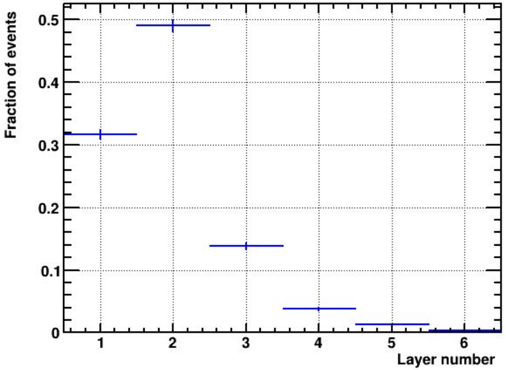

First img layer with registered hit for 5 GeV

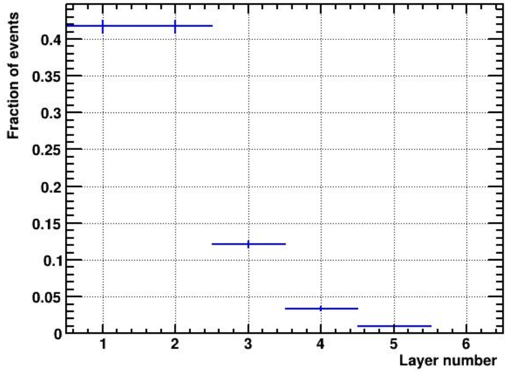

First img layer with registered hit for 10 GeV

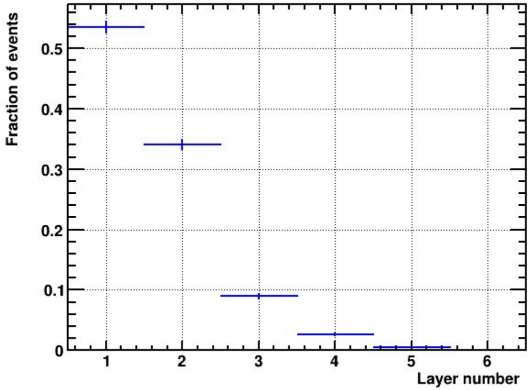

First img layer with registered hit for 20 GeV

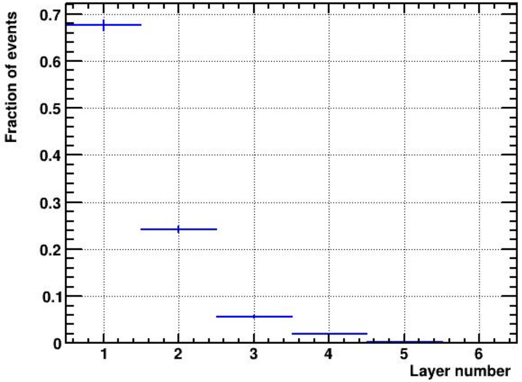

Physics Impact

- Photon physics

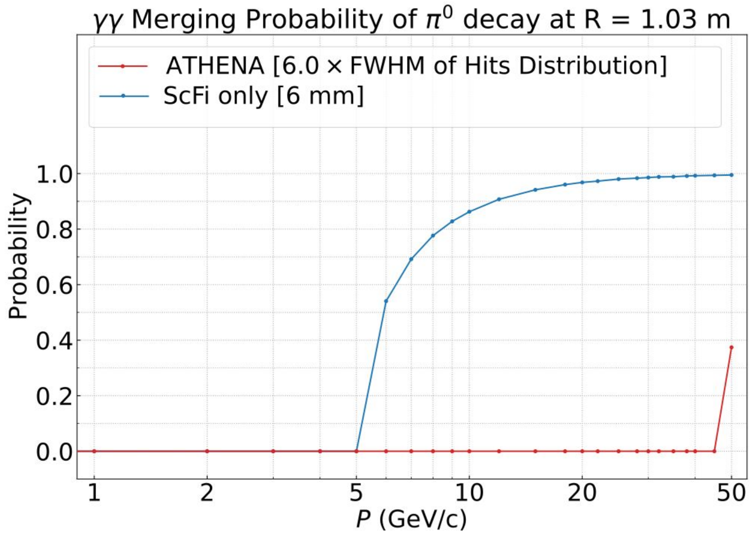

Yellow Report: Separation required up to 20 GeV

Separation between π^0/ɣ

With imaging layers: using 3D shower profile separation of ɣs from π^0 decays at high momenta **up to ~40 GeV/c at R = 1.03 m** and normal incident angle.

With ScFi only:

- Effective cell size of 2 cm × 400 cm
- Separation **driven by timing resolution**. Timing resolution at GlueX results in z-position resolution of the order of 3.1-2.2 cm for neutral showers at 0.5-5 GeV[1]
- In the ideal case for balanced ɣs energy and requiring about 2σ separation (6 cm) between showers - separation **up to ~7 GeV (blue curve)**

Spatial resolution of ɣ

- From imaging layers: of the **order of ~1 mm** (1 GeV ɣ)
- For GlueX ScFi: of the order of **centimeters** from timing resolution (~150 ps for 1 GeV ɣ)

1 See Figure 28 in Nucl. Instrum. Meth. A 896 (2018) 24-42, Construction and Performance of the Barrel Electromagnetic Calorimeter for the GlueX Experiment

NEUTRAL PIONS $\pi^0 \rightarrow \gamma\gamma$

Invariant Mass

- Identify two γs from a neutral pion
  - Position info from imaging layer
  - Energy info from Pb/ScFi layer
- Calibration factor applied to account for slight energy dependence of sampling fraction
- Invariant mass calculated from gammas energy and opening angle

Reconstructed Invariant Mass

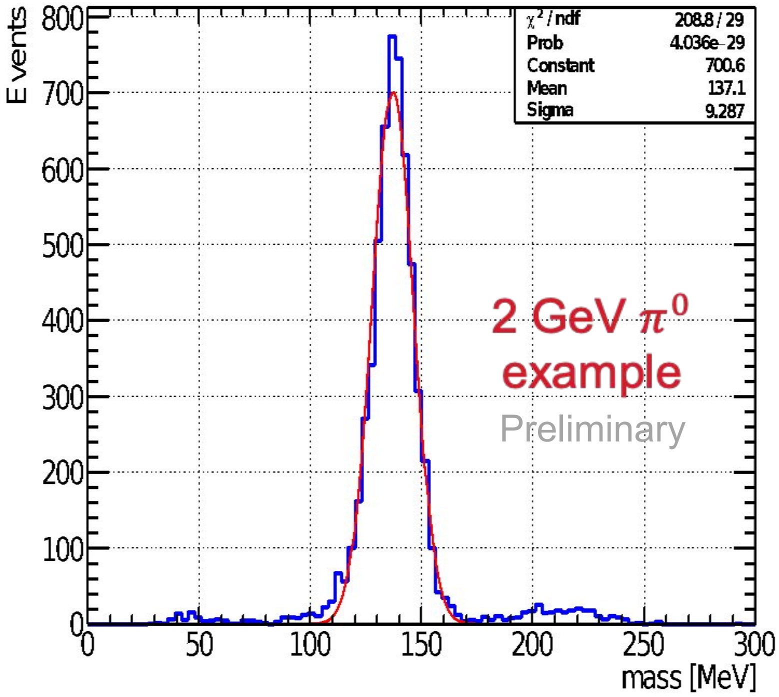

NEUTRAL PIONS $\pi^0 \to \gamma\gamma$

Energy and Position Resolution at Cluster Level

- Reconstruction of π^0 from two γs
- Possible to have even better improvement with first layer hit information

Energy

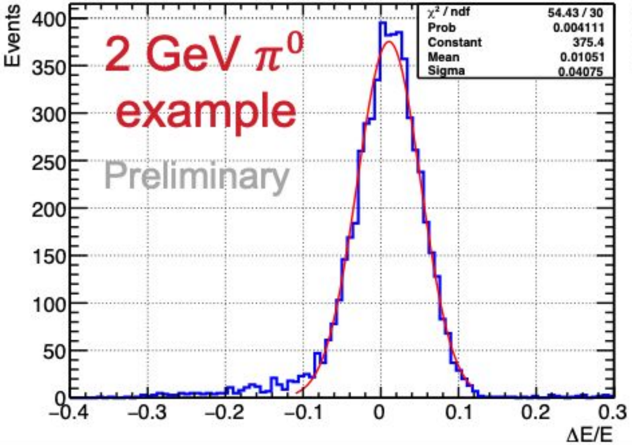

Pseudorapidity

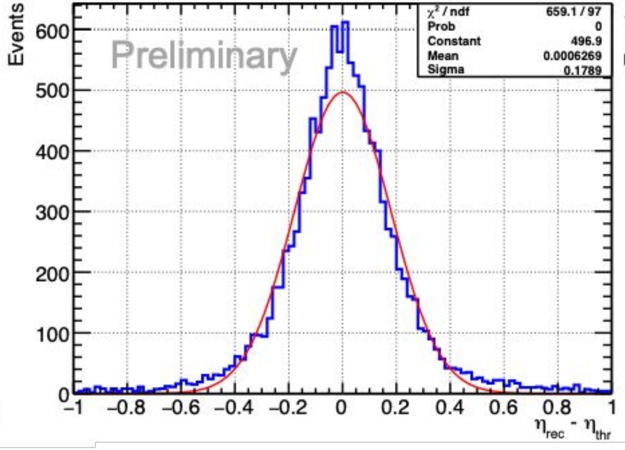

Azimuthal angle

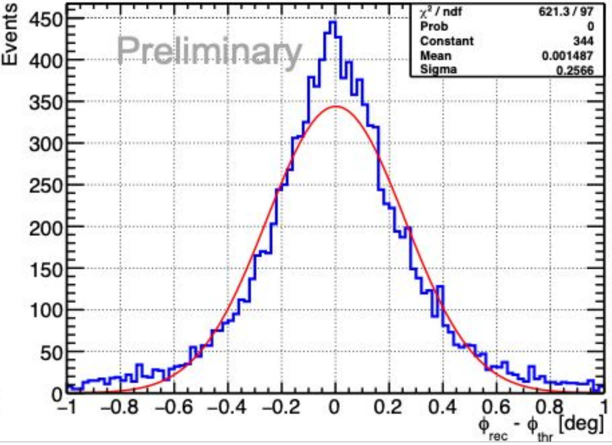

AstroPix

AMEGO-X at NASA

All-sky Medium Energy Gamma-ray Observatory eXplorer

- AMEGO-X operates both as a Compton and pair-production telescope to achieve unprecedented sensitivity between 100 keV and 1 GeV
- Gamma-ray Detector (GRD)
  - Tracker Module (AstroPix), Calorimeter
- Anti-Coincidence Detector (ACD)
  - To reject charge particles (background)

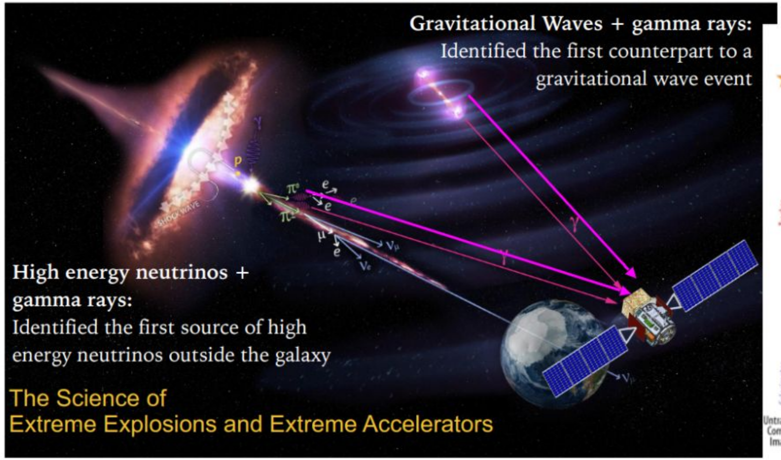

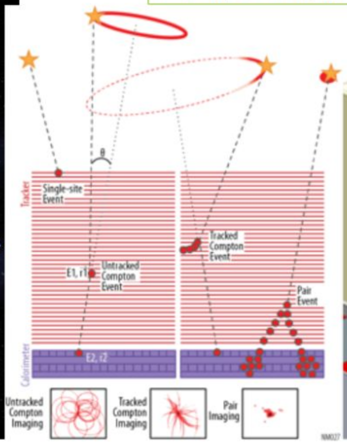

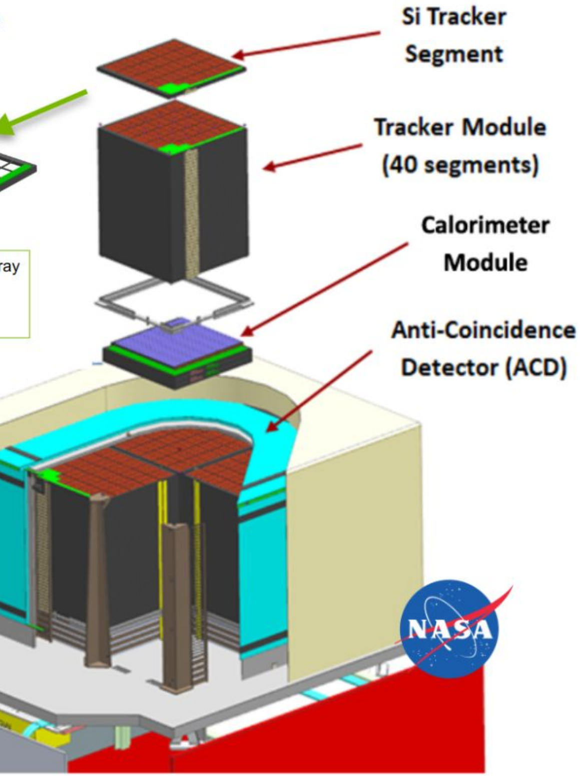

AstroPix for AMEGO-X

AstroPix Sensor

- AstroPix are CMOS sensors based on ATLASPix3 sensors (arxiv:2109.13409)
- AstroPix v1 (4.5 × 4.5 mm² chip)
  - 18 × 18 pixel matrix with 200μm pitch
- Timing resolution ~ 25 ns
- Low power dissipation
- Targeted energy resolution is <10% at 60 keV
- AstroPix v2 is under testing (10 × 10 mm² chip)
  - 35 × 35 Pixel matrix with 250 μm Pixels

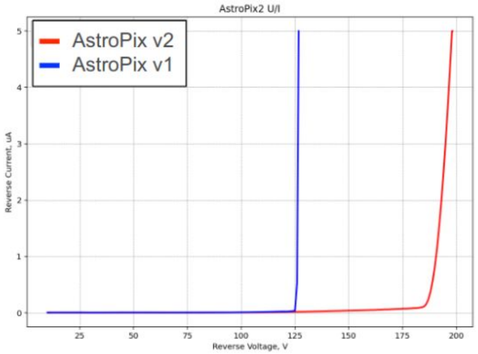

ATLAS-Pix3 Energy Resolution

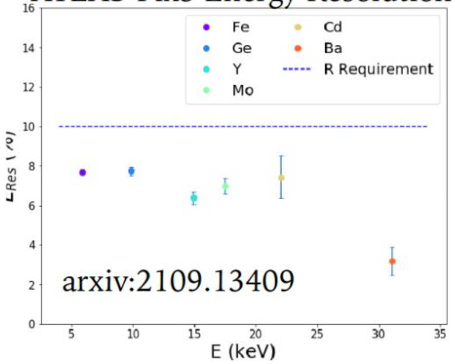

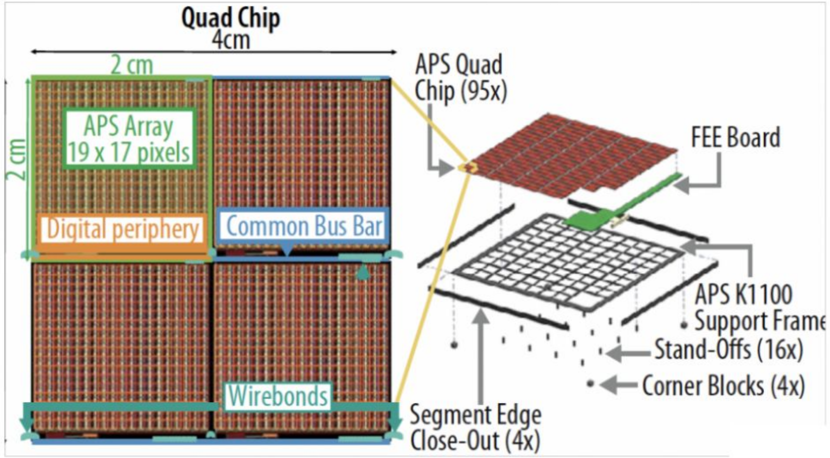

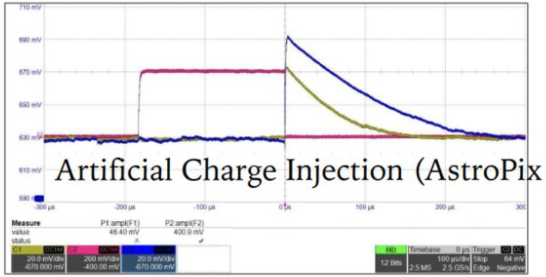

Artificial Charge Injection (AstroPix v1)

AstroPix for AMEGO-X

AstroPix Setup

- **GE**neric **C**onfiguration and **CO**ntrol System (GECCO)
- Connection to FPGA - NexysVideo (Xilinx Artrix-7)
- Vivado Design Suite HLx to program ASIC chip
- Assembly and testing of AstroPix sensors with GECCO boards through FPGA

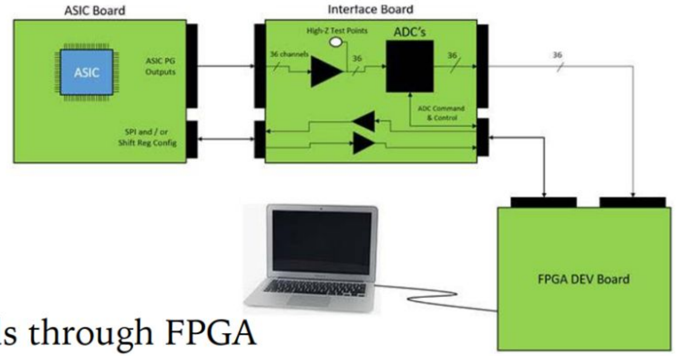

AstroPix-v2 carrier board

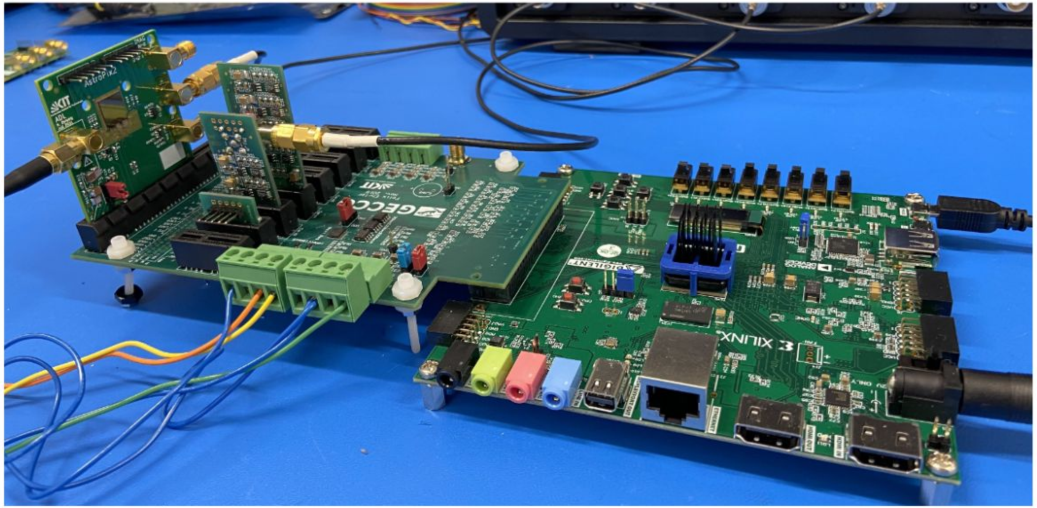

AstroPix for AMEGO-X (V1)

Testing of CMOS sensors

- Data is collected with different γ & β - radiation sources
- Data is analyzed for pulse amplitude distribution and rise time
- AstroPix setup will be integrated with ATLAS telescope planes using HSIO system

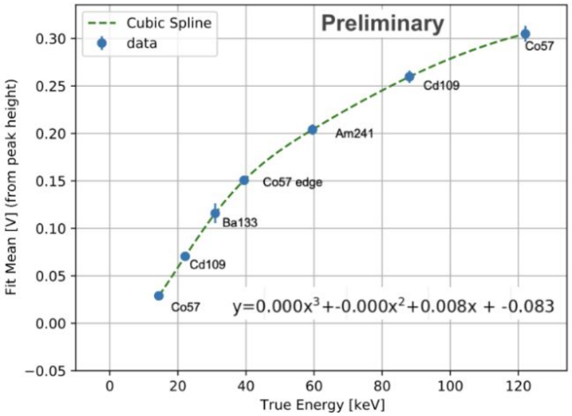

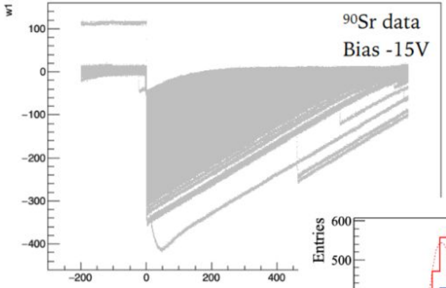

Rise Time (10-90%)

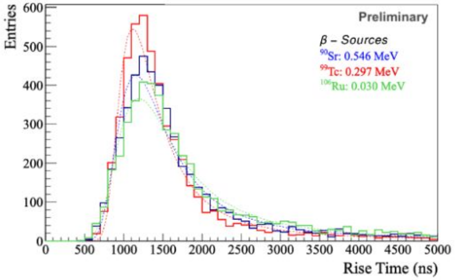

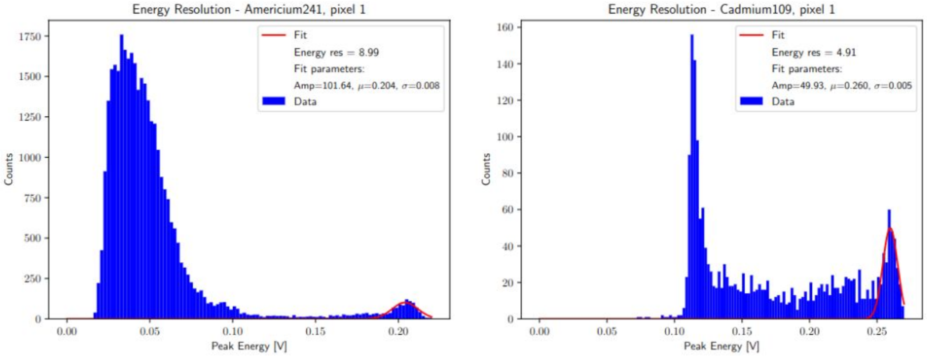

Energy resolution = 2.355* Sigma/mean

AstroPix for AMEGO-X

Testing with 120 GeV proton testbeam

- **AstroPix v2** - 1 cm × 1 cm size chip
- 35 × 35 matrix; 250 μm × 250 μm pixels
- Power dissipation - 5 mW/cm² + Digital (in progress)
- Current study to check latch-ups
- Work in progress: Digital output
    - Digital information; chip ID, pixel location, timestamp, and two bytes for the time-over-threshold (ToT)
- AstroPix v3 is under development

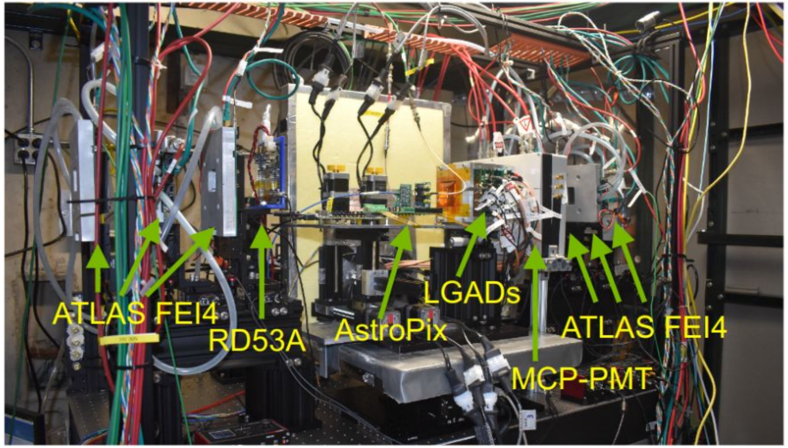


```
Voltageboard settings: [1.1, 1, 0, 0, 1, 1.1, 0, 0]
Digital: {'interrupt_pushpull': 1, 'En_Inj1': 0, 'En_Inj2': 0, 'En_Inj3': 0,
0, 'En_Inj13': 0, 'En_Inj14': 0, 'En_Inj15': 0, 'En_Inj16': 0, 'En_Inj17':
'Extrabit6': 1, 'Extrabit7': 1, 'Extrabit8': 0, 'Extrabit9': 0, 'Extrabit10': 0
Biasblock: {'DisHiDR': 0, 'q01': 0, 'qon0': 0, 'qon1': 1, 'qon2': 0, 'qon3
DAC: {'blres': 0, 'nu1': 0, 'vn1': 20, 'vnfb': 1, 'vnfoll': 10, 'nu5': 0, 'nu6':
'vprec': 30, 'vnrec': 30}
Receiver: {'ColConfig0': 274877906941, 'ColConfig1': 68719476734
68719476734, 'ColConfig6': 68719476734, 'ColConfig7': 687194767
68719476734, 'ColConfig12': 68719476734, 'ColConfig13': 6871947
68719476734, 'ColConfig18': 68719476734, 'ColConfig19': 6871947
68719476734, 'ColConfig24': 68719476734, 'ColConfig25': 6871947
68719476734, 'ColConfig30': 68719476734, 'ColConfig31': 6871947

b'bcbcbcbc2000a5e0b42001a56033bcbcbcbcbcbcbcbcbcbcbcbcbcbcbcbcbcbcbcbcbcbcbcbc
cbcbcbcbcbcbcbcbcbcbcbcbcbcbcbcbcbcbcbcbcbcbcbcbcbcbcbcbcbcbcbcbcbc
cbcbcbcbcbcbcbcbcbcbcbcbcbcbcbcbcbcbcbcbcbcbcbcbcbcbcbcbcbcbcbcbcbc
cbcbcbcbcbcbcbcbcbcbcbcbcbcbcbcbcbcbcbcbcbcbcbcbcbcbcbcbcbcbcbcbcbc
cbcbcbcbcbcbcbcbcbcbcbcbcbcbcbcbcbcbcbcbcbcbcbcbcbcbcbcbcbcbcbcbcbc
Header: ChipId: 0   Payload: 4   Location: 0   Row/Col: Row Tir
Header: ChipId: 0   Payload: 4   Location: 0   Row/Col: Col  Tir
```


bytes

0	1	2	3	4
Header	Hit Location	TS	ToT MSB	ToT LSB

- 0: Frame of 4 Bytes Payload (5 Bytes total)
    - Chip ID in Header
- 1: Hit Location (within the Chip)
    - 1 bit = Row or Column
    - 1 bit Reserved
    - 6 bits Row or Column ID (up to 64 row or column)
- 2: Timestamp
- 3: ToT LSb
- 4: ToT MSb with unused bits in the MSb of that byte


```
b'bcbcbcbc2000a5f0b22001a5f070bcbcbcbcbcbcbcbcbcbcbcbcbcbcbcbcbcbcbcbcbcbcbcbcbcbcbcbcbcbcbcbcbcbcbcbcbcbcbcbcbcbcbcbcbc
bcbcbcbcbcbcbcbcbcbcbcbcbcbcbcbcbcbcbcbcbcbcbcbcbcbcbcbcbcbcbcbcbcbcbcbcbcbcbcbcbcbcbcbcbcbcbcbcbcbcbcbcbcbcbcbcbcbcbcbcbc
bcbcbcbcbcbcbcbcbcbcbcbcbcbcbcbcbcbcbcbcbcbcbcbcbcbcbcbcbcbcbcbcbcbcbcbcbcbcbcbcbcbcbcbcbcbcbcbcbcbcbcbcbcbcbcbcbcbcbcbcbc
bcbcbcbcbcbcbcbcbcbcbcbcbcbcbcbcbcbcbcbcbcbcbcbcbcbcbcbcbcbcbcbcbcbcbcbcbcbcbcbcbcbcbcbcbcbcbcbcbcbcbcbcbcbcbcbcbcbcbcbcbc
bcbcbcbcbcbcbcbcbcbcbcbcbcbcbcbcbcbcbcbcbcbcbcbcbcbcbcbcbcbcbcbcbcbc'
Header: ChipId: 0   Payload: 4   Location: 0   Row/Col: Row Timestamp: 165   ToT: MSB: 15  LSB: 77 Total: 3917 (39.17 us)
Header: ChipId: 0   Payload: 4   Location: 0   Row/Col: Col  Timestamp: 165   ToT: MSB: 15  LSB: 14 Total: 3854 (38.54 us)

b'bcbcbcbc2000a520702001a5c07dbcbcbcbcbcbcbcbcbcbcbcbcbcbcbcbcbcbcbcbcbcbcbcbcbcbcbcbcbcbcbcbcbcbcbcbcbcbcbcbcbcbcbcbcbc
bcbcbcbcbcbcbcbcbcbcbcbcbcbcbcbcbcbcbcbcbcbcbcbcbcbcbcbcbcbcbcbcbcbcbcbcbcbcbcbcbcbcbcbcbcbcbcbcbcbcbcbcbcbcbcbcbcbcbcbcbc
bcbcbcbcbcbcbcbcbcbcbcbcbcbcbcbcbcbcbcbcbcbcbcbcbcbcbcbcbcbcbcbcbcbcbcbcbcbcbcbcbcbcbcbcbcbcbcbcbcbcbcbcbcbcbcbcbcbcbcbcbc
bcbcbcbcbcbcbcbcbcbcbcbcbcbcbcbcbcbcbcbcbcbcbcbcbcbcbcbcbcbcbcbcbcbcbcbcbcbcbcbcbcbcbcbcbcbcbcbcbcbcbcbcbcbcbcbcbcbcbcbcbc
bcbcbcbcbcbcbcbcbcbcbcbcbcbcbcbcbcbcbcbcbcbcbcbcbcbcbcbcbcbcbcbcbcbc'
Header: ChipId: 0   Payload: 4   Location: 0   Row/Col: Row Timestamp: 165   ToT: MSB: 4   LSB: 14 Total: 1038 (10.38 us)
Header: ChipId: 0   Payload: 4   Location: 0   Row/Col: Col  Timestamp: 165   ToT: MSB: 3   LSB: 190 Total: 958 (9.58 us)
```


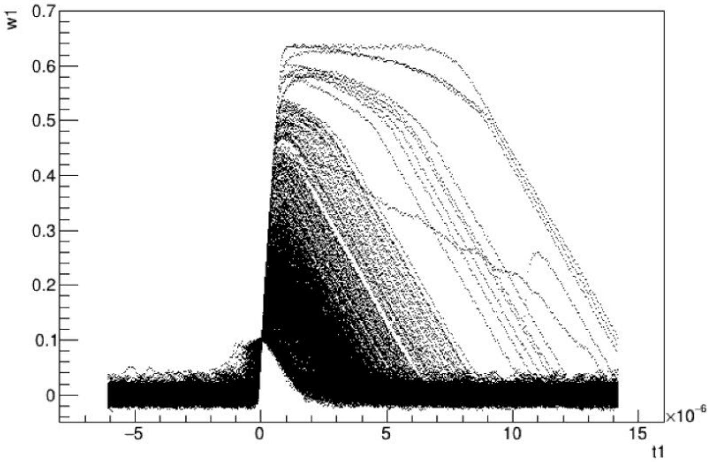

ZONE	REV	DESCRIPTION	DATE	APPROVED

REVISION HISTORY

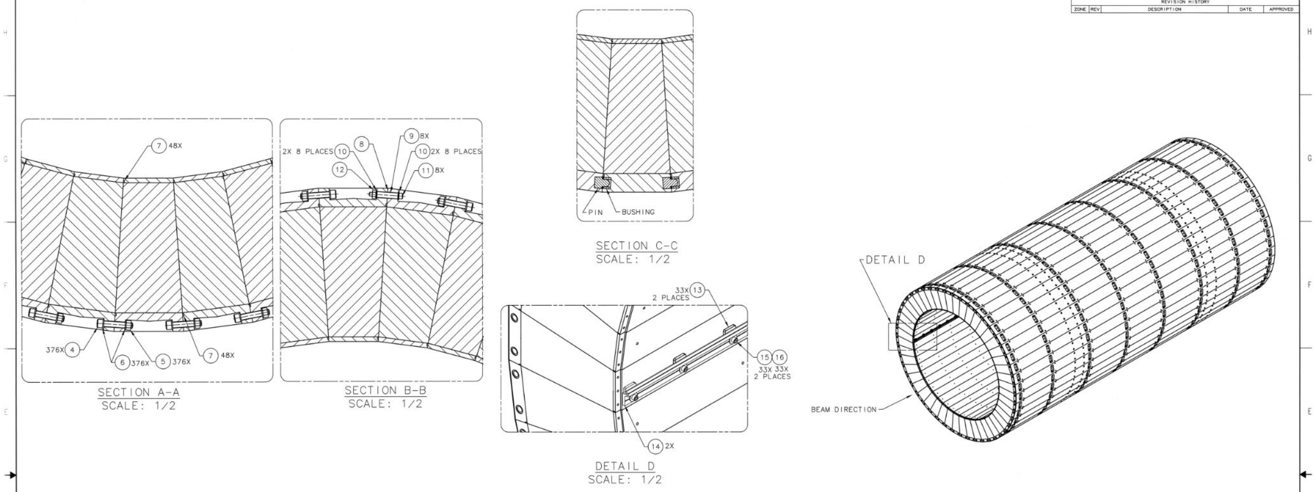

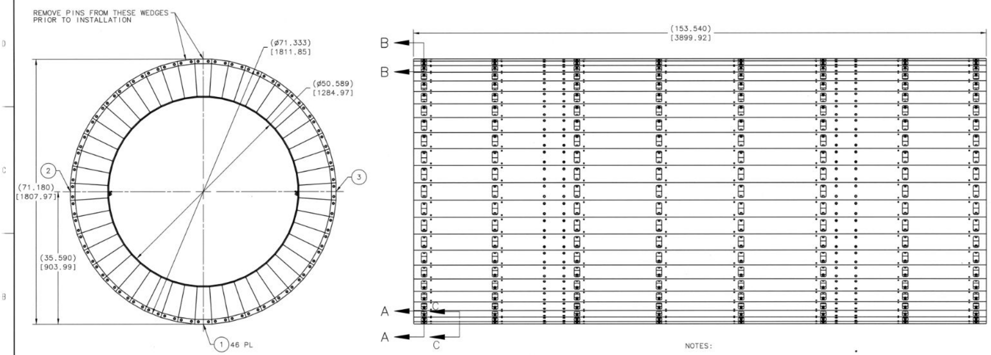

NOTES:

1. SEE BCAL ASSY. PROCEDURE D00000-01-07-P000.
2. ITEM 8 TO BE ATTACHED TO THE NON-ORING SIDE OF WEDGE PLATES. FULL COVERAGE OF WEDGE FACE.
3. SUGGESTED SOURCE OR JLAB APPROVED ALTERNATIVE:

   MCMASTER CARR SUPPLY COMPANY
   (609) 689-3000
   HTTP://WWW.MCMASTER.COM
4. ESTIMATED WEIGHT 57600 LBS.

QTY REQD	ITEM NO.	PART OR IDENTIFYING NO.	NOMENCLATURE OR DESCRIPTION	MATERIAL SPECIFICATION	NOTES
66	16	MCMASTER-CARR 93286A029	FLAT WASHER .25	1100F AL	3
66	15		SOC HD CAP SCREW .25-20 UNC X .75 LG	STAINLESS STEEL TYPE 316	
2	14	D00000-01-07-2006	RAIL		
66	13	D00000-01-07-2007	SPACER		
8	12		HEX NUT .25-20 UNC	SILICON BRONZE	
8	11		SOC HD CAP SCREW .25-20 UNC X 2.00 LG	STAINLESS STEEL TYPE 316	
32	10	MCMASTER-CARR 93493A234	FLAT WASHER .25	FIBERGLASS	3
8	9	D00000-01-07-2008	SLEEVE		
AR	8	MCMASTER-CARR 7648A49	KAPTON TAPE W/ACRYLIC ADHESIVE 6" WIDE X .0025 THICK		2,3
1230'	7	MCMASTER-CARR 9616K12	O-RING CORD STOCK 3/32 DIA.	EPDM	3
752	6	MCMASTER-CARR 98017A200	FLAT WASHER .38	STAINLESS STEEL TYPE 316	3
376	5		HEX NUT .38-16 UNC	SILICON BRONZE	
376	4		SOC HD CAP SCREW .38-16 X 2.00 LG	STAINLESS STEEL TYPE 316	
1	3	D00000-01-07-1003	WEDGE SUB-ASSEMBLY 3		
1	2	D00000-01-07-1002	WEDGE SUB-ASSEMBLY 2		
46	1	D00000-01-07-1001	WEDGE SUB-ASSEMBLY 1		

PARTS LIST

EACH SHEET OF MULTI-SHEET DRAWINGS SHALL ALWAYS HAVE THE SAME REVISION LEVEL.

DOCUMENT CONTROL STAMP: DCG

MATERIAL: SEE PARTS LIST

FINISH MACHINED SURFACES N/A UNLESS OTHERWISE NOTED
DEBURR & BREAK ALL SHARP EDGES

DO NOT SCALE DRAWING

DIM & TOL PER ASME Y14.5. UNLESS OTHERWISE SPECIFIED DIMENSIONS ARE IN INCHES. TOLERANCES ARE: FRACTIONS ± N/A; DECIMAL .X ±.1, .XX ±.01, .XXX ±.005; ANGLES ±.50°

THIRD ANGLE PROJECTION

TRACKING NO. N/A

APPROVALS	DATE
DRAWN J.LAGNER	08FEB08
CHECKED [signature]	16APR09
APPROVED [signature]	16APR09
APPROVED [signature]	16APR09

United States Department of Energy — Jefferson Lab, Thomas Jefferson National Accelerator Facility — Newport News, Virginia

HALL D GLUE-X DETECTOR BARREL CALORIMETER CALORIMETER SUB-ASSEMBLY

SIZE E | DWG. NO. D00000-01-07-1000 | REV. –

SCALE 1:8 | USED ON ASSY NO. D00000-01-07-0000 | SHEET 1 OF 1

Muon PID

Muons in barrel region

- For energies **below ~1.5 GeV/c** muons **curl inside the Barrel ECal**

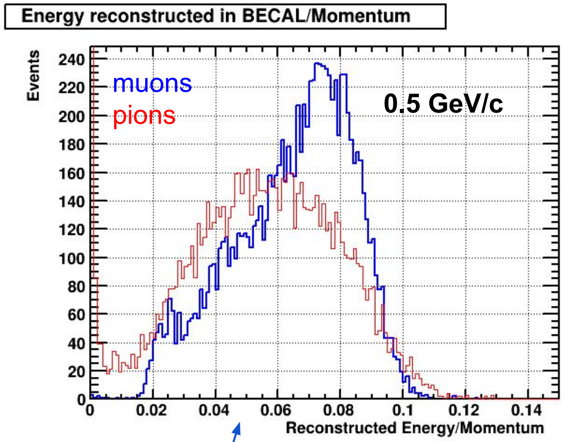

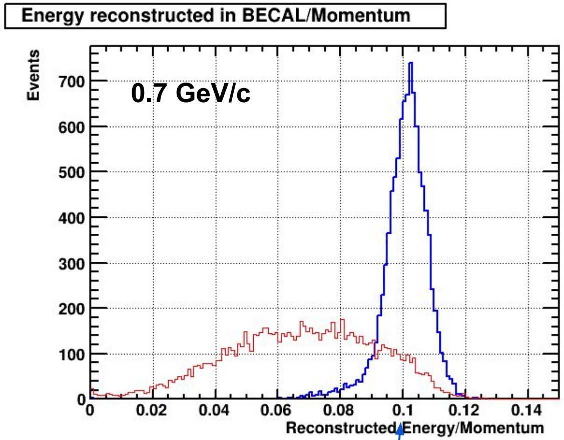

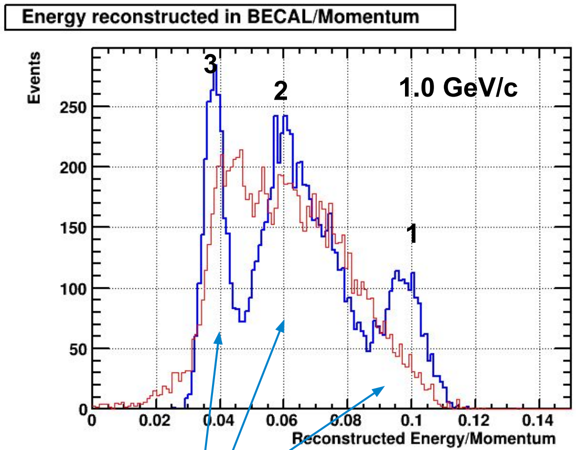

Muons reach only a few first layers of BEcal; deposit partial energy inside the BECal and **curl back**

Muons curl completely inside the BEcal and leave whole energy inside

1. **Muons curl completely** inside the BEcal and leave whole energy inside
2. **Muons punch through** BECal, and **curl back** to stop in BECal
3. **Muons punch through** BECal, and **don't curl back** (MIPs signal)

Sampling fraction of Barrel ECal = ~**0.1**

Muons in barrel region

Example of **muons** and **pions** at **p = 0.5 GeV/c** at η = (-1,1)

Efficiency: 98.9% ⟶ Rejection Power: 6.6

Efficiency: 95% ⟶ Rejection Power: 9.7

Total Energy deposit in ScFi/Pb

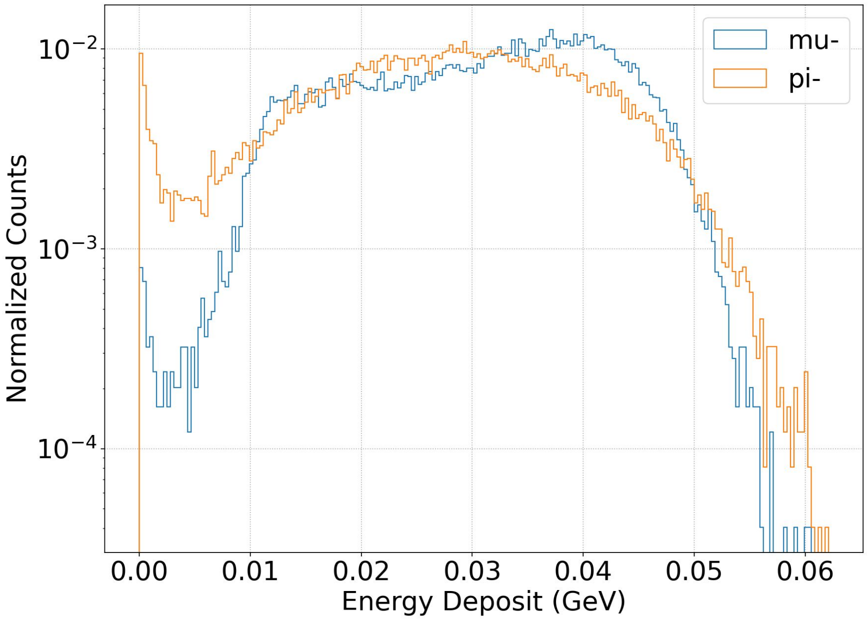

NN output likelihood

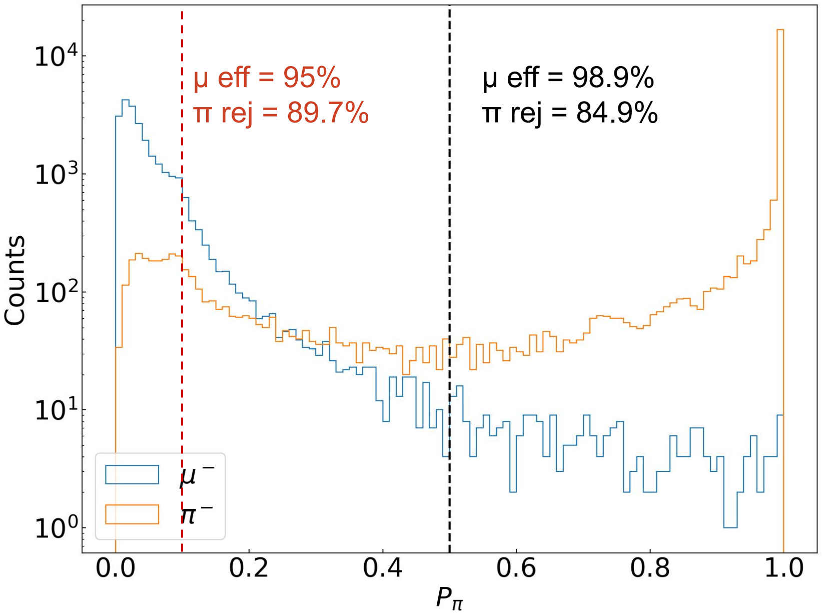

Muons in barrel region

- For energies **below ~1.5 GeV/c** muons **curl inside the Barrel ECal**
- **Barrel ECal with 3T field "serves as" an HCal**

PID Cuts

1) **Method 1:** Using only information from ScFi in Barrel ECal (Energy losses in layers)
   a) Cut on E/p from single ScFi/Pb Calo Layer or sum of all ScFi/Pb Calo Layers

2) **Method 2 (showing impact of imaging layers):** ML supported, using information from **ScFi/Pb and Imaging layers**
   a) Input which encodes the energy and spatial distribution of the particle's shower
      - **Four features** for each hit: η, φ, E, $R = \sqrt{(x^2 + y^2)}$; (no η for ScFi/Pb)
      - Values normalized to [0,1]
      - Three-layers convolutional neural network and three-layers perceptron network
      - Network outputs: **likelihoods** of the input particle to be **identified as a muon or a pion**. Likelihood **cut: 95% of muon efficiency**

Muons in barrel region

Example of **muons** and **pions** at **p = 0.5 GeV/c** at η = (-1,1)
Efficiency: 98.9% ⟶ Rejection Power: 6.6
Efficiency: 95% ⟶ Rejection Power: 9.7

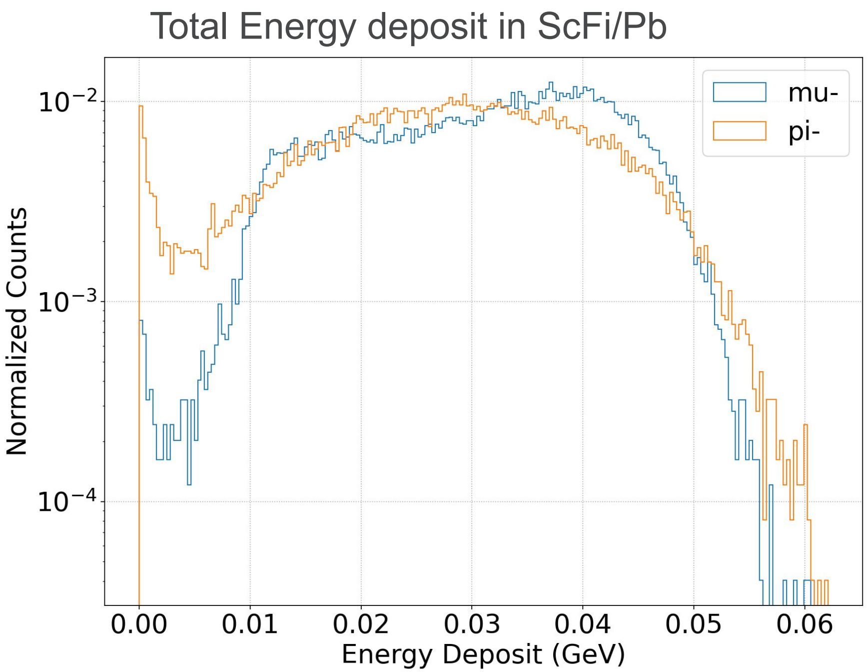

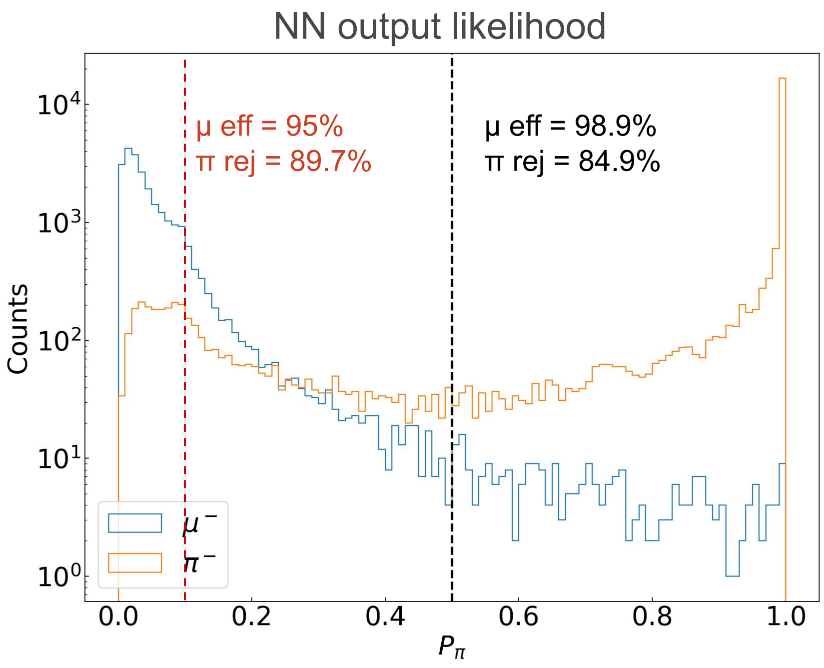

ATHENA Barrel ECal

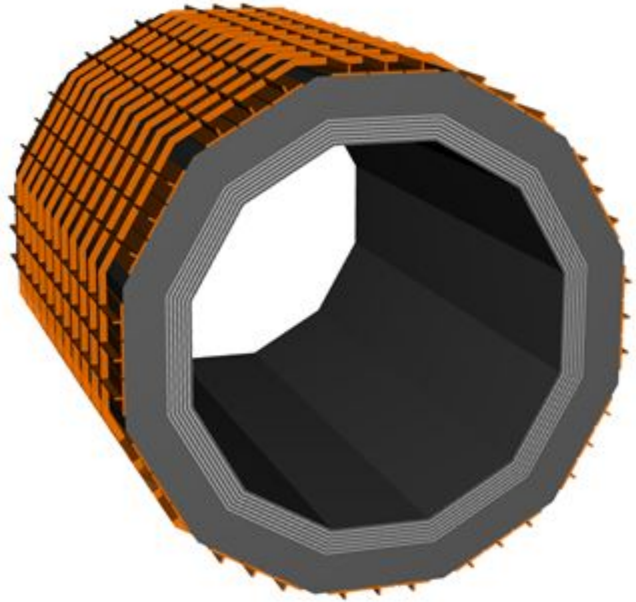

- **Geometry**
  - 12 staves, 6 AstroPix layers (recent adjustment)
  - R_{min} = 1.03 m, Length = 4.05 m, Thickness ~40 cm
  - AstroPix: 1.155 cm per layer (1 cm of air), 1.8% X_0
  - Pb/ScFi: 1.586 cm per layer, ~$1.08X_0$

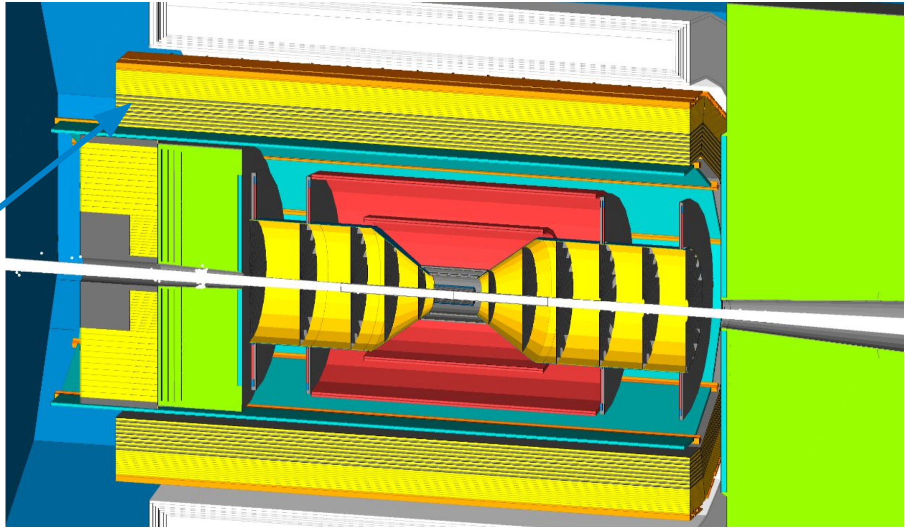

- Contains negative Endcap inside (partially serves as the Endcap detector)

ASTROPIX SENSOR LAYERS

For **6 layers** of imaging layers that cover **$-1.5 < |eta| < 1.2$** the AstroPix sensors area is about **174 m^2**.

Large Si detector arrays in advanced stage (large scale prototypes)

- ATLAS Inner Tracker - silicon strips[1] (ITk pixel) 160 m^2 (50 million channels)
- CMS high granularity calorimeter[2] ~ 600 m^2 (6.5 million channels)

- AstroPix sensors (derived from ATLASpix) will be used in the **AMEGO-X NASA mission**, which is a 40 m^2 experiment sent into space. We expect AstroPix-v3 to be the final version and submitted in spring 2022, and ready in fall 2022.
- We plan to use it off-the-shelf, **meaning with no design modifications**.

Advantages of AstroPix with respect to pixels used in e.g. ATLAS

- AstroPix has very low power consumption (used in space) - 1000 times smaller power consumption per cm^2 than ITk pixel
- AstroPix is a monolithic sensor - less complicated structure
- No bump bonding - less risk of damaging sensors

[1] arXiv:2105.10367, ATLAS ITk Pixel Detector Overview
[2] arXiv:1802.05987, The CMS High-Granularity Calorimeter for Operation at the High-Luminosity LHC2